Developing a Model for Mass Transfer in Adsorption Packed-bed Filters

Golnaz Shaverdi

A Thesis

in

The Department

of

Mechanical and Industrial Engineering

Presented in Partial Fulfillment of the Requirements

for the Degree of Master of Applied Science (Mechanical Engineering) at

Concordia University

Montreal, Quebec, Canada

August 2012

CONCORDIA UNIVERSITY
School of Graduate Studies

This is to certify that the thesis prepared

By: Golnaz Shaverdi

Entitled: Developing a Model for Mass Transfer in Adsorption Packed Bed Filters

and submitted in partial fulfillment of the requirements for the degree of

Master of Applied Science (Mechanical Engineering)

complies with the regulations of the University and meets the accepted standards with respect to originality and quality.

Signed by the final examining committee:

Dr. A.K.W. Ahmed Chair

Dr. I. Hassan Examiner

Dr. C. Mulligan Examiner

Dr. W. Ghaly Supervisor

Dr. F. Haghighat Supervisor

Approved by _____
Chair of Department or Graduate Program Director

_____
Dean of Faculty

Date 09.19.2012

ABSTRACT

Air filtering is an effective approach to maintain the indoor air quality while keeping the building energy consumption at an acceptable range. Adsorption filters are one of the most common types of air purifying devices. One concern about these filters, which inspired much research, is to determine their replacement time, since their efficiency decreases over time during the adsorption process. Therefore, a mass transfer model for adsorption filters had to be developed to predict the decay in filter efficiency over time as a function of the bed properties, the air flow rate, and the adsorbent-adsorbate system characteristics.

This analytical model is validated systematically with experimental results obtained from a small scale and a large scale experimental setup, for two types of contaminants (MEK and n-hexane), at low, middle and high levels of inlet concentration. The model results are then compared with two previously developed models that solve the equations governing mass transfer; one is analytic and one is numerical. The proposed model shows clear advantages over those ones.

Once validated, the model is applied to study the effect of varying four main operating parameters: the convective mass transfer coefficient, the diffusivity within the porous pellets, the air volume flow rate and the pellet size. When studying the effect of varying the air flow rate or the pellet size, the parametric study is carried out in large ranges of Biot number, in order to avoid the influence of convective mass transfer coefficient variations. Indeed it is shown that for large Biot number the controlling parameter is diffusivity within the particles (as anticipated) while, for small Biot number, the convective mass transfer coefficient is the dominant resistance. Finally, the variations of initial efficiency and bed saturation time with respect to changes of these four parameters are discussed.

ACKNOWLEDGMENTS

I would like to express my sincere thanks to my supervisors: Dr. Wahid Ghaly for his valuable suggestions and guiding me in gaining deep knowledge of the problem and Dr. Fariborz Haghighat for his guidance, help and considerate support during my research work.

I am also very grateful to Dr. Change-Seo Lee for teaching me finesse in approaching and analyzing the problem, and her wise feedbacks in laboratory works.

I express my warm thanks to Vida Safari and Arash Bastani who supported me with their extensive experience in this field and my special thanks go to Matin Komeili and Hossein Abdollahi for their great help with the programming language.

I am deeply grateful to Kevin Henriot for his great support all over this work, standing beside me in hard times to be able to find my way and his great advices in writing this report.

At the end I owe my greatest gratitude to my parents, Alireza Shaverdi and Mehrnaz Ajam for their love, support and encouragement.

Table of contents

List of Figures

List of Tables

Nomenclature

English Symbols:

A_s	cross sectional area of the bed [m^2]
A	available surface area of the bed [m^2]
A_p	external surface area of the particle [m^2]
a	available surface area per volume of the bed [m^2/m^3]
a_p	external surface area per unit volume of particle [m^2/m^3]
Bi	Biot number
C_{avg}	average concentration within the pellet [mg/m^3pellet]
C_b	gas concentration in the bulk flow [mg/m^3air]
$\bar{C}_b$	dimensionless gas concentration in the bulk flow
C^*	gas phase concentration adjacent to the surface of the particle in equilibrium with sorbed phase concentration [mg/m^3air]
C^E	ratio of the C^* to the saturation concentration
C_{in}	inlet concentration [mg/m^3air]
C_p	gas phase concentration within the pores of particles [mg/m^3air]
C_{S0}	Maximum monolayer sorbent concentration [mgVOC/m^3AC]

C^{Sat}	concentration in equilibrium with saturation concentration in adsorbent [mg/m^3]
C_e	effluent concentration [mg/m^3]
C_B	breakthrough concentration [mg/m^3]
C_L	operating limit concentration [mg/m^3]
C_0	initial concentration [mg/m^3]
d_p	particle/pellet diameter [m]
d_e	equivalent spherical diameter [m]
dx	length of each section in the bed [m]
D	diffusivity in a single cylindrical pore of the particle [m^2/s]
D_{ax}	axial dispersion coefficient [m^2/s]
D_e	effective diffusivity within the pores of the particle [m^2/s]
D_k	Knudsen diffusivity in pores of the particle [m^2/s]
D_m	molecular diffusion coefficient [m^2/s]
D_s	surface diffusion coefficient [m^2/s]
E_d	linear mass transfer coefficient for the diffusive step [kg/s]
E_h	linear mass transfer coefficient for the convective step [kg/s]
Fo	Fourier number

$\boldsymbol{h_m}$	convective mass transfer coefficient [m/s]
$\boldsymbol{J}$	adsorption amount of a single pellet [mg]
$\boldsymbol{J_i}$	adsorption amount of a single pellet in section *i* [mg]
$\boldsymbol{J_{Bi}}$	total adsorption of all the pellets in the section *i* in the packed bed [mg]
$\boldsymbol{K}$	Linear adsorption isotherm coefficient [m^3Air/m^3AC]
$\boldsymbol{K'}$	Linear adsorption isotherm corresponding to C_{avg} [m^3Air/m^3pellet]
$\boldsymbol{K_{BET}}$	BET adsorption isotherm constant
$\boldsymbol{K_F}$	Freundlich adsorption isotherm constant
$\boldsymbol{K_L}$	Langmuir adsorption isotherm constant [m^3Air/mgVOC]
$\boldsymbol{k_a}$	rate constant of adsorption in BDST model [m^3/mg.s]
$\boldsymbol{L}$	length of the bed [m]
$\boldsymbol{L'}$	characteristic length of the bed [m]
$\boldsymbol{M}$	molecular weight [kg/kgmole]
$\boldsymbol{m}$	$m = \frac{1-\varepsilon_b}{\varepsilon_b}$
$\boldsymbol{M_s}$	mass of adsorbent in the bed [mg]
$\boldsymbol{N}$	number of sections in the packed bed

N_A	mass flux [mg/m^2.s]
N_p	number of particles in the packed bed
N_{pi}	number of particles in each section of the bed
N_0	maximum adsorption capacity [mg/m^3]
n	Freundlich exponent
PD	packing density of the bed [mg/m^3]
Pe	Peclet number
q	volume average sorbed phase concentration of a single particle [mg/m^3]
q_T	Total sorbed phase concentration of all the particles [mg/m^3]
Q	sorbed phase concentration distribution inside the pellets [mg/m^3]
Q_s	sorbed phase concentration at the surface of the pellets [mg/m3]
r	radial distance from center of the spherical particle [m]
r_p	Pore radius [m]
R	gas constant [m^3.Pa / K]
R_p	particle radius [m]
Re	Reynolds number
Sc	Schmidt number

Sh	Sherwood number
T	temperature [K]
t	time [s]
$\bar{t}$	dimensionless time
t_R	Residence time of the bed [s]
t_s	Service time of the bed [s]
u_s	superficial velocity or flow velocity based on empty tube [m/s]
u	interstitial velocity in bed [m/s]
$\dot{V}$	Volume flow rate [m^3/s]
V_b	Volume of the bed [m^3]
V_p	Volume of the particles [m^3]
x	axial distance variable [m]
y	contact time parameter = σt [s]
z	time required for fluid to flow distance x .m [s]

Greek Symbols:

α	distribution ratio = $K.m$
β	fractional surface coverage

γ	$\frac{3D_eK}{{R_p}^2}$ [s]
δ	bed length parameter = $\frac{\gamma x m}{u}$
υ	kinematic viscosity [m^2/s]
ε_b	bed porosity
ε_p	particle porosity
τ	Tortuosity factor
η	dimensionless axial distance variable
θ	time measured from instant point is reached by fluid= t-z/u [s]
ξ	variable of integration
λ_n	characteristic values
υ'	$\gamma \frac{R_p}{3h_m}$
σ	$\frac{2D_e}{{R_p}^2}$ [1/s]
ρ_{air}	air density [mg/m^3]
ρ_{AC}	activated carbon density [mg/m^3]
Δt	residence time in each section [s]
ω	available surface coefficient

Chapter 1: Introduction

1.1. Indoor air quality

The importance of having an efficient heating, ventilation, and air conditioning system in residential, commercial or educational buildings may not be noticed in everyday life. But when these systems stop working, their adverse effect on quality of life, work or other activities starts to be felt very soon. Therefore in order to assure an acceptable indoor air quality (IAQ) and thermal comfort, there is a need for guidelines and standards.

In the past, ventilation standards and guidelines were based on metabolic CO_2 concentration, however nowadays both occupant generated contaminants (e.g., CO_2 or odours) and non-occupant sources such as volatile organic compounds (VOCs) from building materials and furnishings are taken into considerations. The contaminants commonly found indoors are: carbon dioxide, carbon monoxide, ozone, lead, particulates, nitrogen dioxide and VOCs. The American Society of Heating, Refrigerating and Air Conditioning Engineers (ASHRAE) is one of the organization to have set standards for IAQ and thermal comfort (ASHRAE standard 62.1, 2007, ASHRAE standard 55-2004).

ASHRAE standard for an acceptable IAQ prescribes two procedures. The first is the ventilation rate procedure, which specifies the amount of fresh outdoor air that a space needs in terms of air volume per unit time and per person, and which depends on the type of space. This procedure defines the standards for commercial/institutional buildings and low-rise residential buildings. The second procedure is called air quality and it is a performance-based approach, which is based on measuring potential contaminants, analyzing air pollution sources and then determining acceptable level of air pollutants. This method allows for lower amounts of ventilation rate than

with the first procedure when other solutions, e.g. recirculation with air cleaning, are applied to achieve IAQ goals (Charles *et al.* 2005).

One important fact about these procedures is that their associated energy consumption is different. Indeed, when diluting indoor contaminants with fresh outdoor air through ventilation, a large amount of energy is needed to condition the outdoor air. On the other hand, the requirements of ASHRAE standards for buildings with very high occupant densities can create a significant energy burden. As an example, raising the outdoor air flow rate from 2.3 to 7 lit/s increases the (heating) peak loads by 25%-35% in an educational building and by 35%-40% in an auditorium (EPA, 2000). While recirculating the air helps improving the energy efficiency in buildings by reducing the rate of outdoor supply air, such air recirculation is only allowed if the contaminant concentration satisfies a certain criteria (ASHRAE 62.1, 2007).

Air cleaning devices can be used to keep the level of pollutants in an acceptable range hence reducing the ventilation rates and the accompanying energy requirements. There are different types of air filters which are used in HVAC systems to achieve this objective. They can be categorized into particulate (or mechanical) filters, which are used to remove dust and solid particles, and chemical filters, which are used to reduce odors or gaseous pollutants via either an adsorbent or a catalyst. Both the catalyst and adsorption filters usually need to be pre-filtered by particulate filters, as all expensive filters do. In catalysis filters, contaminants are basically decomposed into other compounds; thus sometimes these filters may produce other harmful chemicals. Moreover, the catalyst is deactivated after a while and should then be replaced. By contrast, the adsorption filters are more applicable since they adsorb the contaminants and keep them within the filter. These filters are used extensively for different types of contaminants. An important point about their design is that specific types of adsorbent are suitable for specific

groups of contaminants. By choosing the right adsorbent, considering the physical and chemical characteristics of the adsorbent and the adsorbate, adsorption filters can be designed for various situations. This flexibility is another reason for the widespread usage of adsorption filters for air purification, water treatments and many other separation processes in chemical industries.

Packed bed filters are one of the most common types of adsorption filters. This type of filters consists of a large number of small granules of the adsorbent material, which provide a porous medium with a high surface area allowing for the mass transfer from the fluid to the adsorbent. Sometimes the granules are porous, which increases the adsorption capacity. To design filters of this type, one should take into account many parameters such as: the shape, size and distribution of the granules and packing density of the bed, all of which affect the bed porosity; also the fluid flow rate, the type of adsorbent used, which determines the diffusivity within the granules and the adsorption parameters; as well as others. Thus it is necessary to know how these parameters affect the bed performance.

However, while adsorption filters are efficient, economical and convenient, they saturate after a while, at which point their efficiency decreases and they need to be replaced or in some cases regenerated. To use these filters effectively, one should therefore measure how their efficiency decreases. The efficiency of a filter is defined as the ratio of the adsorption amount and the inlet concentration of the filter. Now, knowing the potential concentration of the contaminants (inlet concentration) and considering the acceptable level of the contaminants concentration according to the IAQ standards (permissible outlet concentration), one can determine the range of filter efficiency. The trend of the variations of efficiency over time then indicates the proper time of filter replacement. Conversely, knowing the replacement time, adsorption filters can be designed. Thus, the first step is to obtain a model that can accurately predict the filter performance. To

achieve this, mass transfer models of adsorption filters have been developed, that predict the contaminant concentration in the fluid at the filter outlet. The input of these models is the inlet fluid conditions and the filter characteristics. The output of these models consists in a plot of the efficiency of the bed versus time, where the efficiency is obtained from the inlet and outlet concentration data. This plot shows the time at which the efficiency (or the outlet concentration) reaches the predetermined point (based on ASHRAE standards) to replace the filter.

Indeed, developing a proper and reliable model for packed bed adsorption filters has been an important issue for many years, with many researchers working in this field and many models being developed for special and general cases. The packed bed mass transfer models that arise repeatedly in the literature are introduced in the literature review. The limitations and validation approaches related to these methods are discussed in the review.

1.2.Objectives

Since there is a need for mass transfer models for packed beds so as to address the limitations and issues mentioned above, we set out the following objectives in this work:

- Develop an efficient and reliable model to quantify the performance of packed bed adsorption filters for a wide range of operation,
- Validate the proposed model against experimental data,
- Using the validated model, carry out a parametric study of a packed bed adsorption filter so as to quantify its performance

1.3. Thesis outline

Chapter 2 is devoted to a literature review whose first aim is to explain the fundamentals of mass transfer in porous media and the governing equations of mass transfer in packed beds and within the particles of the bed, these having a prominent role in the development of the models

introduced later. Its second aim is to introduce certain models that have been developed for mass transfer in packed beds and that are representative of the literature. These have been selected so as to illustrate the different assumptions, simplified approaches and solution methods present in the literature.

Chapter 3 proposes a new model for adsorption in packed beds based on assumptions similar to those used in the existing literature, but featuring a different approach so as to remove certain difficulties encountered in solving the partial differential equations governing the mass transfer in bed and particles simultaneously and avoiding errors in the numerical solution of the relevant differential equations. The fundamental concepts, assumptions, equations, as well as the input parameters used in this model are explained in detail in this chapter.

Chapter 4 is concerned with validating the proposed model: the breakthrough curves obtained from the proposed model are compared with experimental data for different compounds with various inlet concentrations, for large and small scale experimental setups. Following this validation process, a parametric study of the model is carried out to determine the effect of the convective mass transfer coefficient, the diffusion coefficient within the pellets, the volume flow rate and the size of the pellets on the adsorption process in packed beds. Possible sources of error are discussed at the end of this chapter.

Finally, conclusions as well as recommendations for further work on the subject are presented in Chapter 5.

Chapter 2: Literature Review

2.1. Introduction

The literature review in this study is divided into two parts. The first part is about fundamental concepts and the second part is about the different types of models that are developed, applying these fundamental concepts in various ways. The fundamentals are explained in many different ways, which may cause some confusion for the readers. It may even seem that there are some contradictions between different references at first glance and one usually needs a good deal of attention and care to find the consistencies and compatibilities. For example, the use of different symbols is a common source of confusion and may sometimes cause misunderstandings, especially when the writers do not write or use these symbols with enough care. To avoid these issues, a specific symbol is applied for each specific case in this work. However as a result there are many symbols corresponding to different cases. At first this may seem complicated to follow, but eventually it should help to distinguish between the different cases that arise from various assumptions or conditions.

The modeling of mass transfer in packed beds for different kinds of separation processes started six to seven decades ago. Thus a large number of models have been developed for different cases and conditions, and with various assumptions. In this work a few of them are described. It has been the aim of the author to give examples of all kinds of approaches, featuring different assumptions and solving methods.

Packed bed columns can be filled with different types of adsorbents and the mass transfer models for packed beds should be applicable for most of them. However in this work, we restrict our study to adsorption in granular activated carbon filters. Therefore, some specifications of activated carbon are introduced first.

2.2. Activated carbon

The most important characteristic of a sorbent is its high porosity, since the high available surface area of these materials is due to this characteristic. The surface area of activated carbon which is used in this study is between *300* and *2500* m^2/g. It also has a unique surface property: its surface is nonpolar or only slightly polar. As a result it does not adsorb polar groups such as oxide groups or inorganic impurities. Thus it is correct to regard it as hydrophobic (Yang, 1997). This is consistent with the results that show that humidity in the air has little effect on VOC adsorption on activated carbon, especially when the relative humidity is less than 50%. In higher humidity activated carbon filters become less efficient. This is due to the capillary condensation of water vapor within the pores and not to the water vapor adsorption on activated carbon surface. This condensation makes the pores unavailable for adsorbates (Khazraei *et al.* 2011). The pores of gas-phase carbons are mostly in the range of 0.6*nm* -100 *nm* in diameter (measured by micromeritics lab). The pore structure may be pictured as having many micropores (diameters less than 2nm) and mesopores (diameter between 2-50nm) branching off from macropores (diameters more than 50nm), which are open through the entire particle. The larger pores are called feeder or transport pores and the smaller ones, which may be dead-end, are called adsorption pores (Yang, 1997).

2.3. Breakthrough Curves

The performance of packed beds is described through the concept of a breakthrough curve. A breakthrough curve is a plot of the concentration at a fixed point in the bed, usually at or near the outlet, versus time. Alternatively it can be plotted in the dimensionless form by dividing the effluent concentration by the inlet concentration, C_e/C_{in}, so that the vertical coordinate varies

between zero and one, at which point the bed is saturated. Therefore the efficiency of the bed is defined as:

$$\text{Efficiency} = (1 - C_e/C_{in}) \times 100$$

For a constant and continuous input concentration, the breakthrough curve will be *S* – shaped (Figure 2-1). The breakthrough point is the point in the diagram at which the outlet concentration reaches a value predetermined as the air purifying objective. Thus the adsorbent needs to be replaced. This point varies depending on the type of the contaminant. Usually in air or water treatment even a very low amount of contaminant in the effluent is not allowable, therefore the breakthrough point is usually below 5% of the inlet concentration. Most of the time, after this critical point, the outlet concentration increases rapidly.

The breakthrough appearance time and the shape of the curve are very important characteristics for determining the operation and the dynamic response of the sorption column (Goud *et al.* 2005).

2.4. Mass transfer zone

The adsorption process in a packed bed does not occur in the whole bed length during the operation time. In other words a certain length of bed, called mass transfer zone (MTZ), is involved in the adsorption process and it starts moving along the bed, from the inlet point to the outlet point during the operation time. Within the MTZ, the degree of saturation with adsorbate varies from 100% to zero and the fluid concentration varies from the inlet concentration to zero. As the activated carbon in this zone reaches its equilibrium capacity, or in other words becomes exhausted, the MTZ will travel further through the carbon bed. Thus a section of exhausted carbon bed is left behind the MTZ and a section of fresh carbon particles is in front of the

leading edge of the MTZ. When the front edge of the MTZ reaches the end point of the bed, the breakthrough point occurs.

The length of the MTZ is a function of the influent flow rate and the rate of adsorption. If the length of the bed is less than the length of the MTZ, the effluent concentration does not equal zero from the beginning of the process. Besides, the MTZ formation is not instantaneous. It needs a certain time called formation time. Thus if the time of MTZ formation is less than the residence time of the bed, the effluent concentration would again be nonzero at the beginning of the process. Therefore the length and velocity of MTZ are two important factors of adsorption bed design. Minimizing the length of the MTZ increases the capacity of the bed, and this can be used to achieve a predetermined treatment objective (Pure Water Lab Website).

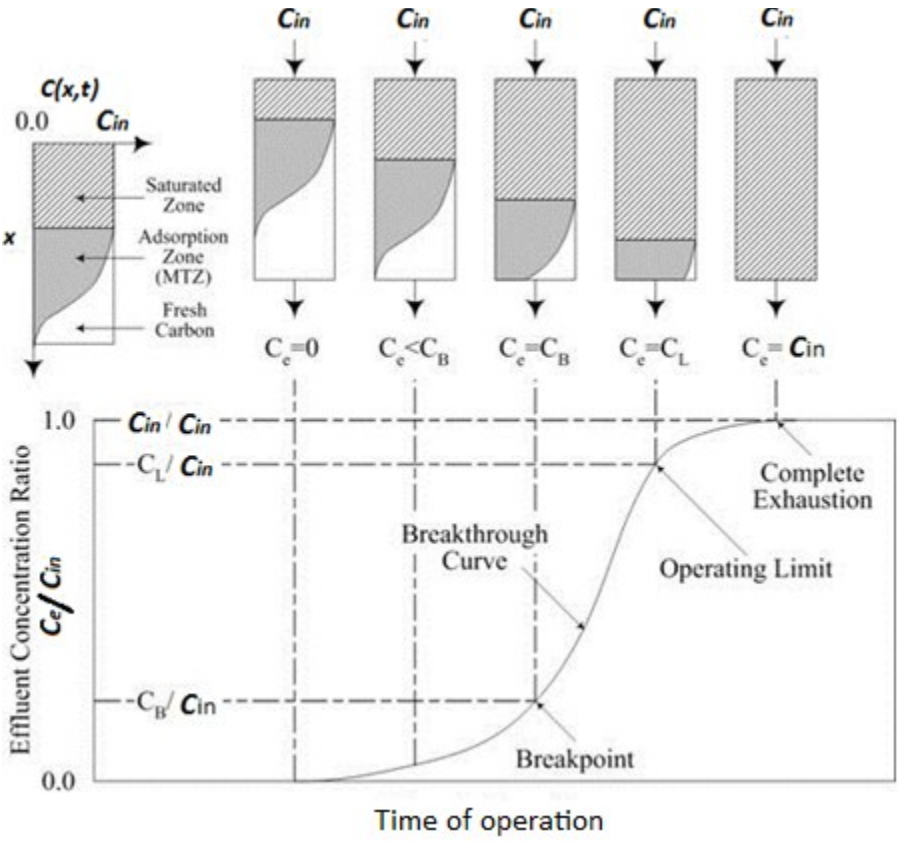

Figure 2-1: Mass transfer zone movement and the corresponding breakthrough curve (from Pure Water Lab website)

Figure 2-1 shows the movement of the MTZ through a carbon bed and the breakthrough curve corresponds to this movement.

2.5. Mass transfer stages

The adsorbate molecules transfer between the fluid and adsorbents through three stages in packed beds. These three stages take place in series and the second one occurs in two parallel mechanisms. They are explained in details in the following.

2.5.1. External transport: First molecules transfer from the bulk flow in the bed to the laminar film adjacent to the particle surface via convection. This step, also called external transport, is represented by the film coefficient h_m, according to the linear law of Fick.

$$N_A = h_m(C_b - C^*) \quad (2\text{-}1)$$

Where N_A is the mass flux, C_b is the bulk concentration and C^* is the gas concentration at the surface of the particle. Different studies have been done on the convective mass transfer coefficient in packed beds (Ranz *et al.* 1952, Thoenes *et al.* 1958, Petrovic *et al.* 1968). Several experiments were also designed to obtain heat and mass transfer coefficient data in packed beds. From this data, accurate and easy to use empirical correlations have been obtained. In this study we use the Wakao-Funazkri correlation; one of the most commonly used correlations, to obtain the convective mass transfer coefficient in packed beds. In 1978, Wakao and Funazkri collected mass transfer coefficient data from studies in packed beds and they limited their collection to works that assume the particles in bed to be all active and the beds to have more than two layers of particles. Among all the studies in liquid phases and gas phases, they chose data of evaporation of water, evaporation of organic solvent, sublimation of

naphthalene, diffusion-controlled reaction on particle surface and dissolution of solid. However in order to avoid the possible natural convection effect, the liquid-phase data for $Re < 3$ was not selected. They computed mass transfer coefficients from this data, correcting it to take into account the axial fluid dispersion coefficient. Indeed some studies had shown that neglecting axial dispersion may cause considerable errors in the evaluation of transfer coefficients, especially at low flow rates and when the fluid is a gas. Axial dispersion effect is explained in section 2.6.1. They suggested the correlation below by plotting $(Sh-2)/Sc^{1/3}$ versus Re for a wide range of Reynolds number 3-10000 (Wakao *et al.* 1978):

$$Sh = 2 + 1.1\, Re^{0.6} Sc^{1/3} \qquad (2\text{- }2)$$

Where Re, Sh and Sc are defined as below in correlation (2- 2):

$$Re = \frac{u_s . d_p}{\nu} \qquad (2\text{- }3)$$

$$Sh = \frac{h_m . d_p}{D_m} \qquad (2\text{- }4)$$

$$Sc = \frac{\nu}{D_m} \qquad (2\text{- }5)$$

where u_s is the superficial velocity, d_p is the pellet diameter, D_m is the molecular diffusivity and ν is the kinematic viscosity of the fluid.

2.5.2. Internal transport: In the second step, the gas molecules penetrate into the porous structure and they are adsorbed on the internal surface of the pellet. The diffusion step occurs through pore diffusion and surface diffusion in parallel. It is important in modeling to recognize which resistance dominates in order to simplify the equations. Therefore the physical process of these transport processes has to be well understood.

- Pore diffusion (Yang, 1997): Diffusion in pores of the particles occurs through two transfer processes depending on the pore size. Molecular diffusion, which results from collisions between molecules, dominates in macropores. Knudsen diffusion occurs for smaller pore sizes due to collisions between molecules and the pore wall. As a rule of thumb, molecular diffusion prevails when the pore diameter is greater than ten times the mean free path of the gas whereas Knudsen diffusion prevails when the mean free path is greater than ten times the pore diameter. The value of the mean free path for air can be calculated, and at 101.3 kPa and 300K it is 2×10^{-5} cm, which is in the range of macropore sizes.

  Since molecular diffusion has the same mechanism as bulk diffusion, the same diffusivity is used for it. The Knudsen diffusivity can be calculated from the equation:

$$D_k = \frac{2r_p}{3}\left(\frac{8RT}{\pi M}\right)^{\frac{1}{2}} = 9700 r_p \left(\frac{T}{M}\right)^{\frac{1}{2}} \qquad (2\text{-}6)$$

  Where D_k is the Knudsen diffusivity, r_p is the pore radius, R is the gas constant, T is the temperature and M is the molecular weight. When the mean free path and the pore diameter are of the same order of magnitude both mechanisms are important. When the mole fraction of adsorbate in the career gas, for example the VOC in air, is very small, the combined diffusion coefficient, D, is obtained as below:

$$D \approx \frac{1}{\left({}^{1}/_{D_m}\right) + \left({}^{1}/_{D_k}\right)} \qquad (2\text{-}7)$$

This diffusion being obtained for a single cylindrical pore, it is not suited for real pore geometry in commercial sorbent particles with complex structures. The effective diffusivity, D_e, in porous material is smaller due to randomness of the pore orientation, connectivity and size variation effects. It can be calculated by different models suggested through extensive studies in this field. For example the simple empirical method, the parallel-pore model, the random-pore model and the dusty-gas model have been proposed (Yang, 1997). In the simple empirical method, the diffusivity is modified for the actual diffusion path as below:

$$D_e = \frac{\varepsilon_p D}{\tau} \qquad (2\text{- }8)$$

The pellet porosity, ε_p, implies that mass transfer occurs only through the pores and not through the solid matrix and that the mass flux given by the effective diffusion coefficient is based on the total cross section of the porous solid (Lee, 2003). The tortuosity factor, τ, is defined as the ratio between the actual diffusion path length and the net distance in the direction of flux, or the radial distance. Since it is a geometric factor, it is independent of temperature and of the nature of the diffusing species. A general correlation for tortuosity shows that it varies inversely with porosity (Ruthven, 1984).

- Surface diffusion: In this diffusion mechanism, molecules hop between adsorption sites. Thus the surface diffusivity, D_s, has a strong dependence on the surface concentration and the fractional surface coverage. In fact it becomes dominant when both the surface area and the surface concentration are high. In adsorptive gas separation processes both these conditions are

satisfied. For example in the diffusion of methane, ethane and ethylene in activated carbon at 20°C and pressure below 0.2 atm, the contribution of the surface diffusion to the total flux ranges approximately between 40% and 80% (Yang, 1997). Also the surface diffusion should depend on temperature since the hopping mechanism is an activated process. Therefore the surface diffusivity varies consequently for different cases depending on the adsorbate concentration and the temperature, and it should be studied and calculated in each particular case. For example, Masamune *et al.* (1964) found that pore diffusion is dominant at liquid nitrogen temperature *-196°C,* for nitrogen adsorption on Vycor glass r_p=*5Å,* while surface diffusion is dominant for the same process in room temperature *20°C*. The limited literature data for the surface diffusion coefficient may have caused the neglecting of the surface diffusion in many models (Pei *et al.* 2010). Do *et al.* (2001) obtained the surface diffusivity at zero loading (β=0), at reference temperature 303K for propane, n-butane and n-hexane in activated carbon. The order of magnitude of D_s for these compounds is 10^{-10}- 10^{-12} m^2/s which is negligible against pore diffusion. But it is important to notice that the surface diffusivity increases when the sorbed phase concentration (loading) increases and one cannot neglect it without considering the adsorption conditions. Yang et al. (2003) used a concentration-dependent surface diffusivity correlation in their model. Different types of correlations have been introduced by researchers that show the behavior of surface diffusivity versus sorbed phase concentration (Higashi *et al.* 1963, Neretnieks, 1976, Kapoor *et al.* 1991, Miyabe *et al.* 1997).

In conclusion, it is important to know which mechanism is dominant in the mass transfer process through the particle and which resistance is controlling. Different models have been developed assuming different conditions in the mass transfer equations: homogeneous surface diffusion model, pore diffusion model, pore surface diffusion model, etc. These models for mass transfer within the particles are explained in 2.6.2.

2.5.3. Adsorption: When the adsorbate molecules reach the interface between the gas phase and the solid phase, either at the external surface or within the pores of the particles, the adsorbate molecules can attach to the sorbent molecules via physical or chemical adsorption. Physical adsorption involves the weak van der Waals forces and electrostatic interactions, thus the inverse of the process, desorption, may also happen. The formation of a physically adsorbed layer may be like the condensation of vapor to liquid. In chemical adsorption the bond between the sorbate and sorbent forms via electron transfers, therefore it is an activated mechanism which involves a high heat of adsorption and may be irreversible. (Ruthven 1984, Young 1962). In this work we consider physical adsorption in packed bed filters.

2.6. Mathematical models of adsorption in packed beds

Mathematical models predict the performance of adsorption filters under specific conditions. They can also be useful in designing areas. In designing we need to decide about bed specifications such as the length and cross sectional area of the bed, the type and size of the particle, the amount of particles (bed porosity) and the operational conditions.

Different models have been introduced by researchers. Some of them are discussed later in this chapter (Section 2.7). The assumptions and conditions vary, but mostly three main equations have been applied in developing these models.

1. The mass and heat balance equations for the bulk gas in the bed
2. The mass and heat balance equations within the particles
3. The adsorption isotherm equation

The resistance to heat and mass transfer both inside and outside the sorbent pellet, can be important, depending on the operational conditions, one of them is sometimes neglected in favor of the other. The models usually assume that the local rate of adsorption is instantaneous compared to transport processes.

2.6.1. Mass balance equation for the bulk gas in the bed

The mass balance equation for the bulk flow in the bed, neglecting radial dispersion, is:

$$-D_{ax}\frac{\partial^2 C_b(x,t)}{\partial x^2}+\frac{\partial(uC_b(x,t))}{\partial x}+\frac{\partial C_b(x,t)}{\partial t}+\frac{1-\varepsilon_b}{\varepsilon_b}\frac{\partial q_T(x,t)}{\partial t}=0 \qquad (2\text{-}9)$$

Where D_{ax} is the axial dispersion coefficient, u is the interstitial velocity in bed, x is the axial distance variable, t is the time, ε_b is the bed porosity and q_T is the total sorbed phase concentration of all the pellets.

Boundary conditions for $t>0$:

$$C_b(0,t)=C_{in} \qquad (2\text{-}10)$$

$$\frac{dC_b(L,t)}{dx}=0 \qquad (2\text{-}11)$$

where C_{in} is the inlet concentration. Initial condition for $0<x<L$:

$$C_b(x,0)=0 \qquad (2\text{-}12)$$

Figure 2-2 shows the gas flow through a packed bed.

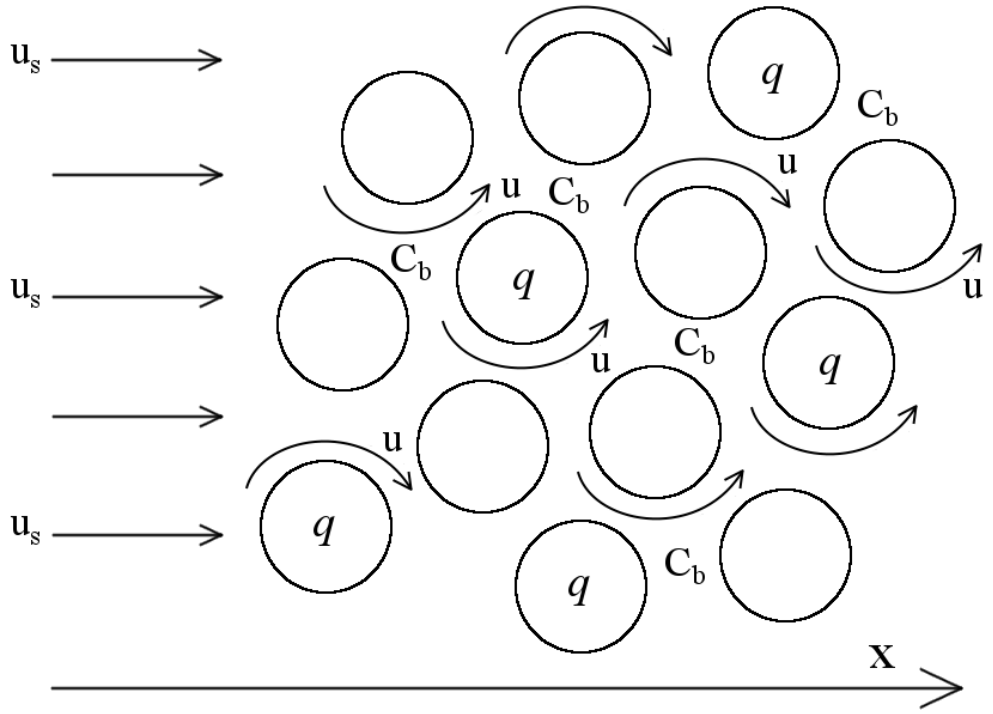

Figure 2-2: Gas flow through a packed bed

In this PDE we have the following terms:

- Diffusion term ($-D_{ax}\ \frac{\partial^2 C_b}{\partial x^2}$) :

  Axial mixing is an undesirable term while the fluid flows through the packed bed since it reduces the efficiency of the separation process. Therefore choosing proper bed and flow conditions to minimize this term is important in order to improve the separation factor in the bed.

  The presence of the axial dispersion coefficient, D_{ax}, shows that the effect of all the mechanisms contributing to axial mixing. Molecular diffusion and turbulent mixing are identified as two main mechanisms that cause axial mixing for a uniform packed bed (Ruthven, 1984). Depending on the velocity ranges, either molecular diffusion or turbulent mixing becomes dominant. The Peclet number describes axial dispersion in the

gas flow through packed beds. Wakao and Funazkri (1978) used the equations below to obtain the dispersion coefficient.

- For evaporation, sublimation, dissolution or a diffusion controlled chemical reaction taking place at the particle surface, under the condition that the inside of the particle is not involved in the mass transfer or the chemical reaction process:

$$\frac{\varepsilon_b D_{ax}}{D_m} = 20 + 0.5\, Sc\,.\,Re \qquad (2\text{-}13)$$

$$Pe = \frac{D_{ax}}{u d_p} = \frac{20}{Sc\,.\,Re} + 0.5 \qquad (2\text{-}14)$$

- Under the inert condition, which means that no mass transfer takes place between the particles and fluid in packed beds:

$$\frac{\varepsilon_b D_{ax}}{D_m} = (0.6 - 0.8)\varepsilon_b + 0.5\, Sc\,.\,Re \qquad (2\text{-}15)$$

None of the conditions above exactly fits the adsorption process in packed beds, but one can use the first equation with some error to obtain the axial dispersion coefficient.

Although the diffusion term is neglected against the advection term in most of the models, it should be noted that this is only possible under certain specific conditions. These conditions are explained in Section 2.6.4.

One should note that the second boundary condition is only necessary when the diffusion term is not neglected (second order differential equation). Some models use other boundary conditions for the end of the bed, for example:

$$C_b(\infty, t) = 0 \quad \text{Or} \quad \frac{d^2 C_b(L,t)}{dx^2} = 0 \qquad (2\text{-}16)$$

- Advection ($\frac{\partial u C_b}{\partial x}$) :

  This term represents the transport of the substances due to the fluid's bulk motion in the axial direction (Contaminants are carried by the airflow passing through the filter). The interstitial velocity, u, is the fluid velocity inside the bed among the particles and is correlated to the superficial velocity as below:

$$u = \frac{u_s}{\varepsilon_b} \tag{2- 17}$$

- Accumulation/dissipation ($\frac{\partial C_b}{\partial t}$) :

  This term is the transient term which accounts for the accumulation/dissipation of substances during time.

- Sink of the process ($\frac{\partial q_T}{\partial t}$):

  This term is the adsorption, which basically shows mass transfer from the gas phase to the solid phase. The rate of adsorption is obtained in various ways such as quasichemical, linear rate-fluid film, linear rate-solid film, solid diffusion models, etc. In this study we use the linear rate-fluid film model. Based on this model, the relation between the sorbed phase concentration for a single particle, q, and the gas phase concentration in the bulk is as below, since the mass transfer rate of convection from the bulk to the gas layer adjacent to the particle surface is assumed equal to the rate of adsorption inside the pellet.

$$\frac{\partial q(x,t)}{\partial t} = h_m . a_p . \left(C_b(x,t) - C^*(x,t)\right) \tag{2- 18}$$

  Where a_p is the external surface area per unit volume of the particle. The gas phase concentration in the laminar film adjacent to the surface of each particle, C^*, is in

equilibrium with the sorbed (solid) phase concentration at the surface of the particle, Q_s, and the relation between C^* and Q_s, is given by the adsorption isotherm correlation.

It should be noted that to obtain the total adsorption rate for particles in the bed at the position x and time t, the available surface area per volume of the bed, a, should be considered:

$$\frac{\partial q_T(x,t)}{\partial t} = h_m.a.\left(C_b(x,t) - C^*(x,t)\right) \quad (2\text{- }19)$$

2.6.2. Mass balance equation within the particles

Concerning the diffusion inside the grain, three classes of models have been proposed:

- Homogeneous Surface Diffusion Model (HSDM): In the HSDM, porous particles are considered as a pseudo-homogeneous medium. It is assumed that the contaminants adsorb at the external surface of the particles and then diffuse within the particles (Richard *et al.* 2010).

$$\frac{\partial Q(r,x,t)}{\partial t} = D_s\left[\frac{1}{r^2}\frac{\partial}{\partial r}\left(r^2\frac{\partial Q(r,x,t)}{\partial r}\right)\right] \quad (2\text{- }20)$$

Boundary and initial conditions:

$$\frac{\partial Q(0,x,t)}{\partial r} = 0 \quad (2\text{- }21)$$

$$h_m(C_b(x,t) - C^*(x,t)) = D_s\frac{\partial Q(R_p,x,t)}{\partial r} \quad (2\text{- }22)$$

$$Q(r,x,0) = 0 \quad (2\text{- }23)$$

Where Q is the sorbed phase concentration within the pellet, r is the radius distance and R_p is the pellet radius. For simplification, we use $q(x,t)$, an average value of the sorbed phase concentration, $Q(r,x,t)$, over the volume of the particle, in the linear rate-fluid film model. It is calculated as below:

$$q(x,t) = \frac{\int_0^{R_p} Q(r,x,t) r^2 dr}{\int_0^{R_p} r^2 dr} \quad (2\text{- }24)$$

- Pore Diffusion Model (PDM): This model assumes that the contaminant diffuses through the pores of the particles and then adsorbs on the internal surface of the particle (Richard *et al.* 2010).

$$\frac{\partial C_p(r,x,t)}{\partial t} + \frac{1-\varepsilon_p}{\varepsilon_p}\frac{\partial Q(r,x,t)}{\partial t} = D_e\left[\frac{1}{r^2}\frac{\partial}{\partial r}\left(r^2\frac{\partial C_p(r,x,t)}{\partial r}\right)\right] \quad (2\text{- }25)$$

Where C_p is the gas phase concentration within the pores of the pellet. Some models neglect adsorbate accumulation in the gas phase within the pores of the particles and write equation (2- 25) as below:

$$\frac{1-\varepsilon_p}{\varepsilon_p}\frac{\partial Q(r,x,t)}{\partial t} = D_e\left[\frac{1}{r^2}\frac{\partial}{\partial r}\left(r^2\frac{\partial C_p(r,x,t)}{\partial r}\right)\right] \quad (2\text{- }26)$$

Boundary and initial conditions:

$$\frac{\partial C_p(0,x,t)}{\partial r} = 0 \quad (2\text{- }27)$$

$$Q(r,x,0) = 0 \quad (2\text{- }28)$$

$$C_p(r,x,0) = 0 \quad (2\text{- }29)$$

$$h_m(C_b(x,t) - C^*(x,t)) = D_e\frac{\partial C_p(R_p,x,t)}{\partial r} \quad (2\text{- }30)$$

It is important to note that the diffusivity is different in the HSDM and the PDM. The diffusivity in the HSDM is based on the solid phase concentration gradient and the diffusivity in the PDM is the effective pore diffusivity (Yang, 1997).

- Pore Surface Diffusion Model (PSDM): It assumes that both phenomena occur simultaneously. This model is more complicated and the type of equations that arise is

different. Choy *et al.* (2001), Hand *et al.* (1998) developed their models considering both the pore and surface diffusion mechanism within the particles.

$$\varepsilon_p \frac{\partial C_p(r,x,t)}{\partial t} + \left(1-\varepsilon_p\right)\frac{\partial Q(r,x,t)}{\partial t} = \varepsilon_p D_e \left[\frac{1}{r^2}\frac{\partial}{\partial r}\left(r^2 \frac{\partial C_p(r,x,t)}{\partial r}\right)\right] + (1-\varepsilon_p) D_s \left[\frac{1}{r^2}\frac{\partial}{\partial r}\left(r^2 \frac{\partial Q(r,x,t)}{\partial r}\right)\right] \quad (2\text{-}31)$$

Boundary and initial conditions (Noll *et al.* 1992):

$$\frac{\partial C_p(0,x,t)}{\partial r} = 0 \qquad \frac{\partial Q(0,x,t)}{\partial r} = 0 \quad (2\text{-}32)$$

$$h_m(C_b(x,t) - C^*(x,t)) = \varepsilon_p D_e \frac{\partial C_p\left(R_p,x,t\right)}{\partial r} + (1-\varepsilon_p) D_s \frac{\partial Q\left(R_p,x,t\right)}{\partial r} \quad (2\text{-}33)$$

$$Q(r,x,0) = 0 \quad (2\text{-}34)$$

$$C_p(r,x,0) = 0 \quad (2\text{-}35)$$

2.6.3. Adsorption Isotherm equations

Equilibrium isotherm or adsorption isotherm models assume that at a constant temperature, the solid phase and the adjacent gas are in equilibrium and the amount of adsorbate on the solid phase is a function of the gas concentration.

$$C_{sorbedphase} = f(C_{gasphase}, T) \quad (2\text{-}36)$$

In other words,

For the HSDM we can write: $C^* = f^{-1}(Q_s) \quad while \quad Q_s = Q(R_p,x,t)$ (2- 37)

For the PDM we can write: $C_p(r) = f^{-1}\left(Q(r)\right) \; while \quad C_p\left(R_p\right) = C^*$ (2- 38)

Thus the adsorption isotherm equation is the link between the gas and sorbed phase concentrations in the mathematical models of adsorption in packed beds. There have been

various types of adsorption isotherm equations and the most commonly applied are (Noll *et al.* 1992):

- The linear adsorption isotherm is the simplest adsorption isotherm and is a special case for adsorption of Henry's law defining the discontinuity in concentration at a two-phase interface. According to Henry's law at a constant temperature, the amount of a given gas that dissolves in a given type and volume of liquid is directly proportional to the partial pressure of that gas in equilibrium with that liquid. This is restated for any other two-phase interfaces like solid-gas in adsorption: at a constant temperature, the amount of a given gas that adsorb in a given type and volume of adsorbent is directly proportional to the concentration of that gas in equilibrium with that adsorbent. Thus the partition coefficient is the same as the linear adsorption isotherm constant. Equation (2- 39) shows the linear adsorption isotherm equation. Here the adsorption isotherms are written according to HSDM.

  $$Q_s = KC^* \tag{2- 39}$$

  Where K is the linear adsorption isotherm coefficient. The linear adsorption isotherm coefficient is found experimentally for each pair of adsorbate-adsorbent system.

- The Freundlich adsorption isotherm correlates the sorbed phase concentration to the gas phase concentration via a power function. This equation is valid when there is no chemisorption, in other words sorbate molecules that do not change in the adsorbed state and whose adsorption process is completely physical. Equation (2- 40) shows the Freundlich equation.

  $$Q_s = K_F C^{*1/n} \tag{2- 40}$$

The Freundlich adsorption isotherm constant, K_F, and the Freundlich exponent, n, are also obtained empirically for each pair of adsorbate-adsorbent system. In high concentration, the Freunlich equation does not show a limit and predicts that the adsorption amount increases to infinity with the gas concentration. In low concentrations the Freunlich isotherm does not reduce to the linear isotherm.

- The Langmuir adsorption isotherm can be applied for chemisorption too. Five assumptions are made to derive the Langmuir adsorption isotherm: ideal adsorbed gas, monomolecular layer adsorption, homogeneous surface with the same affinity for all the binding sites, no interaction between adsorbed molecules and localized stationary adsorbed gas molecules. Equation (2- 41) shows the Langmuir adsorption equation.

$$Q_s = \frac{C_{s0} K_L C^*}{1 + K_L C^*} \qquad (2\text{- }41)$$

In the above, the maximum monolayer sorbent concentration, C_{S0}, is a constant independent of temperature and the Langmuir adsorption isotherm constant, K_L, is a constant depending on temperature, and these constants are found experimentally for each pair of adsorbate-adsorbent system. This correlation converges to a limiting amount of C_{S0} for high levels of gas concentration and reduces to the linear adsorption isotherm for low levels of gas concentration.

- The BET adsorption isotherm was developed by Brunauer, Emmett, and Teller in 1938. They extended Langmuir's model to multilayer adsorption by assuming that each molecule adsorbing in the first layer provides one site for the second and subsequent layers. Molecules which are not in the first layer are not in contact with the surface of the adsorbate, therefore they behave as a saturated liquid with a different equilibrium

constant than the first layer. Equation(2-42) shows the BET adsorption isotherm equation.

$$Q_s = \frac{C_{s0} K_{BET} C^E}{(1 - K_{BET} C^E)(1 - C^E + K_{BET} C^E)} \quad (2\text{-}42)$$

Where: $$C^E = \frac{C^*}{C^{sat}} \quad (2\text{-}43)$$

K_{BET} is the BET adsorption isotherm constant and C^{sat} is the concentration in equilibrium with saturation concentration in adsorbent. This expression shows a good agreement with the experimental adsorption isotherm data for C^E between 0.35-0.5.

2.6.4. Non-dimensional equations

Making equations dimensionless is useful to get a better idea about the effect of each term in the PDEs, to see which part of the equation is negligible against other parts and to determine what the conditions should be for these assumptions.

In order to non-dimensionalize the equations we first have to find the scale of each term. Here we use the following scales to make the physical quantities non-dimensional:

$$C_b \sim C_{in} \longrightarrow \overline{C_b} = \frac{C_b}{C_{in}} \quad (2\text{-}44)$$

$$x \sim L' \longrightarrow \eta = \frac{x}{L'} \quad (2\text{-}45)$$

$$\tau' \sim \frac{L'^2}{D_{ax}} \longrightarrow \bar{t} = \frac{t}{\tau'} \quad (2\text{-}46)$$

$\overline{C_b}$, η, $\bar{t}$ are the dimensionless gas concentration in the bulk fluid, axial distance variable and time respectively. The characteristic length of the bed, L', is defined as below (Whitekar, 1972):

$$L' = \frac{d_p . \varepsilon_b}{(1 - \varepsilon_b)} \quad (2\text{-}47)$$

Neglecting the velocity gradient along the bed, equation (2-9) becomes non-dimensional as follows:

$$-\frac{\partial^2 \overline{C_b}}{\partial \eta^2} + Re'.Sc'.\frac{\partial \overline{C_b}}{\partial \eta} + \frac{1}{m^2}\frac{\partial \overline{C_b}}{\partial Fo'} + a.L'.Sh'.\overline{C_b} = a.L'.Sh'.\frac{f^{-1}(Q_s(x,t))}{C_{in}} \quad (2\text{- }48)$$

Where the dimensionless numbers are given by:

$$m = \frac{1-\varepsilon_b}{\varepsilon_b} \quad (2\text{- }49)$$

$$Re' = \frac{u.L'}{\nu} = \frac{u_s.d_p}{(1-\varepsilon_b).\nu} \quad (2\text{- }50)$$

$$Sc' = \frac{\nu}{D_{ax}} \quad (2\text{- }51)$$

$$Fo' = \frac{D_{ax}.t}{L'^2} = \frac{D_{ax}.t}{{d_p}^2} \quad (2\text{- }52)$$

$$Sh' = \frac{h_m.d_p}{D_{ax}} \quad (2\text{- }53)$$

The prime in *Re′, Sc′, Fo′, Sh′* indicates that these dimensionless numbers are obtained through the non-dimensionalization of the bed PDE. Thus the axial dispersion coefficient appears in their correlations. From the non-dimensional equation, we can see that if $Re' \cdot Sc'$ is much larger than one (say at least 10 times larger), we can neglect the diffusion term against the advection term.

2.7. Variant models for packed beds

As mentioned before, various models have been developed making different assumptions and applying different equations (HSDM, PDM, etc) and solution methods to predict the breakthrough curves of packed bed adsorption filters. Since we develop a model for packed beds in this study, it is relevant to explain these first in order to compare them with the proposed model.

Models for packed beds usually start from the partial differential equations of the fluid in the bed and of the particles. Thus under various assumptions, one obtains different types of PDEs and

applying different methods to solve them, one obtains different models. In the following several models are explained that use analytical or numerical methods to solve the PDEs.

2.7.1. Analytical Models

- Rosen (1952):

  The Rosen model is explained here in detail since it gives an analytical solution that has been used in many studies. It is therefore useful to study this model carefully to understand at what conditions it is valid. Rosen made the assumptions below to write the mass balance equations.

  1. The diffusion term in the bed mass balance equation is neglected because it is assumed to be much smaller than the advection term.
  2. The convective mass transfer coefficient and the solid diffusion coefficient are independent of position and concentration over the range of its variation.
  3. The system has a linear isotherm so that under equilibrium conditions, the concentration of adsorbed material at the surface of the solid is given by $Q_s=KC^*$.
  4. A uniform liquid surface film surrounds each solid spherical particle and the concentration at the outer surface of this film is that in the body of the fluid, C_b. It seems that Rosen did not consider the contacts between pellets and assumed that the available surface area of the bed is equal to the sum of the surface areas of all the pellets.
  5. The particles are small enough so that the change in concentration over a length equal to the particle diameter can be neglected.

The PDE in the inter-pellet air phase is the same as equation (2- 9) without the diffusion term and assuming constant velocity along the bed.

$$\mathrm{u}\frac{\partial C_b}{\partial \mathrm{x}}+\frac{\partial C_b}{\partial \mathrm{t}}=-\frac{1-\varepsilon_\mathrm{b}}{\varepsilon_\mathrm{b}}\frac{\partial \mathrm{q}}{\partial \mathrm{t}} \tag{2- 54}$$

Rosen also did the following change of variable to obtain equation (2- 56).

$$z=\frac{1-\varepsilon_b}{\varepsilon_b}\frac{x}{u} \quad , \quad \theta=t-\frac{x}{u} \tag{2- 55}$$

$$\frac{\partial C_b}{\partial z}=-\frac{\partial q}{\partial \theta} \tag{2- 56}$$

The boundary and initial conditions are the same as mentioned before in equations (2- 10), (2- 12) and Rosen considered the linear rate-fluid film for the rate of adsorption as mentioned in equation (2- 18).

When writing the mass balance equation within the particles, Rosen uses the HSDM. For the second boundary condition of the HSDM he writes:

$$Q\left(R_p,z,\theta\right)=Q_s(z,\theta) \tag{2- 57}$$

Thus the linear rate-fluid film along with using linear adsorption isotherm yields:

$$\frac{\partial q}{\partial \theta}=\frac{3h_m}{R_p}\left(C_b-\frac{Q_s}{K}\right) \tag{2- 58}$$

Rosen solved equations (2- 56) , (2- 58) analytically and obtained the solution in the form of an infinite integral which is a function of only three dimensionless parameters $\gamma z, \sigma\theta, \nu'$:

$$\frac{C_b(z,\theta)}{C_{in}}=\frac{1}{2}+\frac{2}{\pi}\int_0^\infty e^{-\gamma z H_1(\xi,\nu')}\times sin[\sigma\theta\xi^2-\gamma z H_2(\xi,\nu')]\frac{d\xi}{\xi} \tag{2- 59}$$

Where: $\gamma=\frac{3D_eK}{{R_p}^2}$, $\nu'=\gamma\frac{R_p}{3h_m}$, $\sigma=\frac{2D_e}{{R_p}^2}$ (2- 60)

$$H_1(\xi,\nu')=\frac{[H_{D1}+\nu'\,({H_{D1}}^2+{H_{D2}}^2)]}{[(1+\nu' H_{D1})^2+(\nu' H_{D2})^2]} \tag{2- 61}$$

$$H_2(\xi,\nu')=\frac{H_{D2}}{[(1+\nu' H_{D1})^2+(\nu' H_{D2})^2]} \tag{2- 62}$$

$$H_{D1}(\xi) = \xi\left(\frac{sinh\,2\xi + sin\,2\xi}{cosh\,2\xi - cos\,2\xi}\right) - 1 \qquad (2\text{- }63)$$

$$H_{D2}(\xi) = \xi\left(\frac{sinh\,2\xi - sin\,2\xi}{cosh\,2\xi - cos\,2\xi}\right) \qquad (2\text{- }64)$$

The results of this model will be discussed further in Chapter 4.

- Rasmuson & Neretnieks (1980):

Rasmuson and Neretnieks extended the Rosen equation for the general case in which the diffusion term is not neglected. This is also explained here in detail in order to compare with the case of Rosen. Their assumptions in developing the model are as below (Bobcock *et al.* 1966):

1. Homogeneous, unconsolidated pack.
2. Uniform flat velocity profile.
3. Negligible radial concentration gradient in the bed.
4. The physical properties of both phases are temperature independent for any given set of conditions.
5. The particle diameter is small enough so that the concentration gradietn across a single particle due to longitudinal fluid gradients does not influence the concentration distribution within the particle, that is, radial symmetry exists within the individual spherical particles.
6. The system has a linear isotherm.

Therefore the PDE in the bed is the same as equation (2- 9). In this model the PDE of the bed needs two boundary conditions to be solved since it is of second degree. The first boundary condition and the initial condition are the same as in Rosen's model, but Rasmuson & Neretnieks write the second boundary condition as follows:

$$C_b(\infty, t) = 0 \qquad (2\text{-}65)$$

The mass balance equation within the particles is written using the HSDM as in Rosen's model. The analytical solution is obtained in a way similar to that of Rosen, and the infinite integral is again given as an explicit function.

$$\frac{C_b(x,t)}{C_{in}} = \frac{1}{2} + \frac{2}{\pi}\int_0^{\infty} \exp\left(\frac{1}{2Pe} - \sqrt{\frac{\sqrt{(F^2+G^2+F}}{2}}\right) \sin\left(y\xi^2 - \sqrt{\frac{\sqrt{(F^2+G^2-F}}{2}}\right) \frac{d\xi}{\xi} \qquad (2\text{-}66)$$

Where: $$m = \frac{1-\varepsilon_b}{\varepsilon_b} \qquad (2\text{-}67)$$

Bed length parameter: $$\delta = \frac{\gamma x m}{u} \qquad (2\text{-}68)$$

Distribution ratio: $$\alpha = Km \qquad (2\text{-}69)$$

Peclet number: $$Pe = \frac{xu}{D_{ax}} \qquad (2\text{-}70)$$

Contact time parameter: $$y = \sigma t \qquad (2\text{-}71)$$

$$F = Pe\left(\frac{1}{4}Pe + \delta H_1\right) \quad , \quad G = \delta Pe\left(\frac{2}{3}\frac{\xi^2}{\alpha} + H_2\right) \qquad (2\text{-}72)$$

The other parameters are the same as in Rosen's model. The results of this equation are to be compared with the results of Rosen in Chapter 4 to see the effect of the diffusion term.

2.7.2. Numerical Models

- Popescu, Blondeau, Jouandon & Cola (2007):

This model is described in detail as an example to illustrate one of the approaches of numerical models. To develop this model:

1. Isothermal conditions are assumed and the Langmuir adsorption isotherm is applied.

2. It is assumed that the sorbed phase concentration, Q, remains in equilibrium with the pore air phase concentration, C_p.

In addition, they defined the linear driving force model applied for the contaminant convection from the bulk gas to the gas laminar layer at the surface of the pellet. The mass transfer coefficient for this step, E_h, is defined as:

$$E_h = \rho_{air}.a.h_m \qquad \text{where } \rho_{air} \text{ is the air density} \qquad (2\text{- }73)$$

They also defined the linear driving force model applied for the contaminant diffusion in the porous pellets, considering the difference between the contaminant concentration at the pellet surface and the pore gas-phase concentration within it (C_p) as a driving force. The mass transfer coefficient for this step, E_d, is defined according to linear driving force (LDF) model as:

$$E_d = \frac{15\ M_s D_e K}{R_p^2} \qquad (2\text{- }74)$$

Where M_s is the mass of adsorbent in the bed and K is linear adsorption isotherm coefficient. The PDE of the bed is of the general form introduced in equation (2- 9), and for the mass balance equation within the pellets, the PDM is applied (equation (2- 25)).

To solve the PDEs, the filter is decomposed into n elemental cells connected in series and the concentrations C_b, C^*, C_p and Q are assumed to be uniform within a same cell. The PDEs for the bed and the pellets are then discretized and rewritten for each cell in the bed. Since the flux of the mass transfer is assumed to be identical for the convective step and the diffusive step, Popescu et al. conclude that the rate of adsorption in the equations can be written as below:

$$E_h(C_b - C^*) = E_d\left(C^* - C_p\right) = E_d\left(C^* - f^{-1}(q)\right) = \frac{E_h E_d}{E_h + E_d}\ (C_b - f^{-1}(q)) \qquad (2\text{- }75)$$

The discretized equations are then solved simultaneously using the dynamic system simulation program Matlab/Simulink.

Axial dispersion is not neglected in the bed mass balance equation at the first step. However in the discretized equations the recirculation factor, which shows the possible air recirculation between adjacent cells, is considered equal to zero, which means that the flow is assumed to be an ideal plug flow.

Popescu *et al.* (2007) also extend their model for the mixture of contaminants using the extended Langmuir equation. The model is eventually run for six contaminants pertaining to different chemical classes with each gas isolated first, and then with all the gases in the mixture with 50 elemental cells. The results are in agreement, although not completely satisfactorily, with experiments for some single gases in certain ranges of E_d and E_h. For the mixture of contaminants the breakthrough curves do not fit the experimental data for all six contaminants.

Some other numerical models are explained briefly in the following:

- Bautista *et al.* (2003) studied the adsorption of α-amylase in a fixed bed of Duolite XAD-761. They developed a mass transfer model for adsorption in packed beds considering the external-film model and the pore diffusion model (PDM) mass transfer mechanisms. They did not neglect the axial dispersion term. Using the Langmuir adsorption isotherm, they solved the set of PDEs numerically by reduction to a set of ordinary differential equations using the orthogonal collocation method. The model results were then compared to experimental data. However the model parameters such as h_m and D_e were not computed according to the bed conditions and experimental conditions, but rather they were chosen so as to fit the results of the mathematical model to the experimental breakthrough curves.

- Babu and Gupta (2005) take into account both the external and internal mass transfer resistances. They use the PDM for the intra-particle mass transfer and they consider a non-ideal plug flow along the column to account for the variation of fluid velocity along the column, resulting the following mass balance equation:

$$\frac{\partial(uC_b(x,t))}{\partial x} = u\frac{\partial C_b(x,t)}{\partial x} + C_b(x,t)\frac{\partial u}{\partial x} \qquad (2\text{-}76)$$

Babu and Gupta used the Langmuir adsorption isotherm and solved the equations numerically by reduction to a set of ordinary differential equations using the explicit finite difference technique. Their model was not validated by experimental data either. Their results were compared with those of the previous model (Bautista *et al.,* 2003) using the same parameters as theirs. The effect of velocity variation on the breakthrough curve was studied (Figure 2-3). Moreover, the effects of operating variables such as flow rate, bed height, inlet adsorbate concentration and particle diameter on the adsorption in packed beds were also studied.

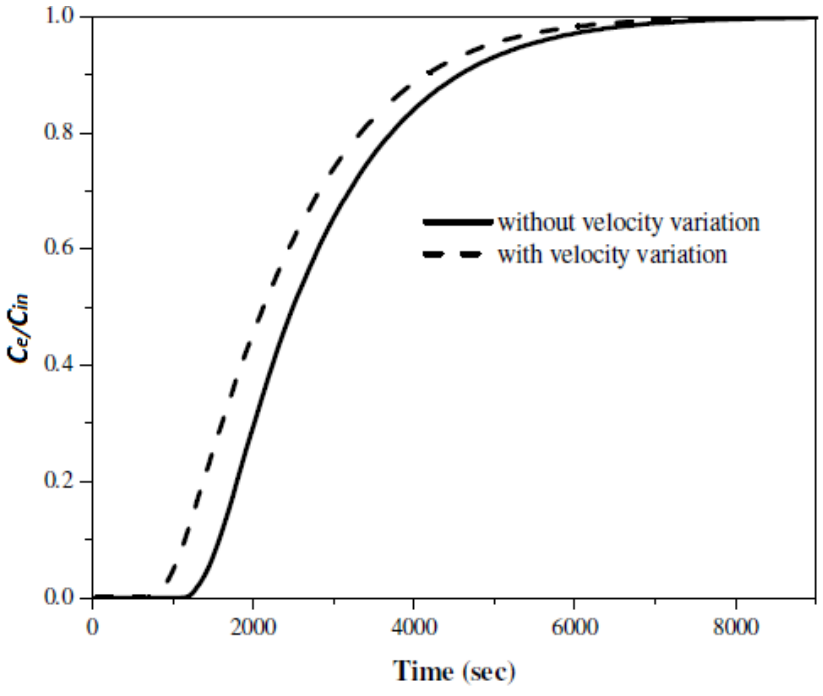

Figure 2-3: Breakthrough curve with and without fluid velocity variation (from Babu *et al.*, 2005)

- Chang *et al.* (2006) used the analytical solution discussed by Klinkenberg for the simplified form of the mass balance PDE, neglecting the axial dispersion term, considering a constant fluid velocity, and using the linear driving force model and the linear adsorption isotherm. By fitting the experimental breakthrough curves to the analytical solution of Klinkenberg, the coefficient of overall mass transfer (which includes both the external and internal mass transfer) was determined. The external mass transfer coefficient, h_m, was then calculated from the Wakao-Funazkri correlation. Thus the internal mass transfer coefficient, D_e, could be found using the overall and external mass transfer coefficients. The analytical solution of Klinkenberg cannot predict the breakthrough well for different inlet concentrations because the breakthrough curve remains almost the same for various inlet concentrations. This is the same problem as encountered in the models of Rosen and Rasmuson & Neretnieks and it is discussed in Chapter 4.

2.7.3. Another type of models

The bed depth service time model (BDST) is a different approach introduced first by Bohart and Adams (1920). This model neglects both the external and internal mass transfer resistances (Inglezakis *et al.* 2006). It is simple, rapid and applicable to predict the effect of different inlet concentrations and bed depth and flow rates on the fixed bed performance. However its validity is limited to a certain range of conditions, for example to a specific range of breakthrough (Singh and Pant, 2006). The BDST model assumes that the service time, t_s, for a determined breakthrough concentration, C_B, and the height of the bed, L, are correlated with the process parameters such as maximum adsorption capacity, N_0 and rate constant of adsorption in BDST model, k_a:

$$t_s = \frac{N_0}{C_{in} u_s} L - \frac{1}{k_a C_{in}} \ln\left(\frac{C_{in}}{C_B} - 1\right) \quad (2\text{-}77)$$

In this study we do not explain this model in detail since the approach of this study is different from the one there. However it should be noted that many studies have been done on the BDST model. A few recent ones are mentioned here.

- Zhao and Ducan (1998) studied the adsorption of zinc ions on a biosorbent from Azolla filiculoides. The BDST parameters were obtained for this system. Moreover the BDST model was shown to be applicable for this system under specific conditions. However the data was limited to predict service time and bed height for varying flow rates.
- Singh and Pant (2006) did an experimental study on the adsorption of arsenic ions from an aqueous solution in an activated alumina fixed bed to determine the effect of some parameters such as fluid velocity, length of the bed, inlet concentration, etc. They also compared their experimental results with two types of packed bed models, the pore diffusion model (PDM) and the bed depth service time model (BDST), and obtained the model parameters.
- Sze *et al.* (2008) studied the adsorption of organic pollutants by activated carbon in tapered columns. The BDST original model was then modified according to the experimental data for tapered columns.
- Ramesh *et al.* (2011), Balci *et al.* (2011) have also done studies on different adsorbent-adsorbate systems, applying BDST and other types of empirical models. Yin *et al.* (2009) and Walker *et al.* (1997) used the BDST model for an adsorption system with activated carbon as adsorbent.

Chapter 3: Methodology

3.1. Introduction

The aim of modeling the mass transfer in packed bed filters is to predict the breakthrough time according to the goals of the separation process. Different models have been developed for different adsorption systems; they usually start from the partial differential equation (PDE) governing the pollutant mass transfer in the packed bed, as explained in Chapter 2. The model proposed in this study will be presented and explained in this chapter. In contrast with other models, this model starts with the mass transfer within a single porous pellet and extends it to include the whole bed. The fundamental concepts, assumptions and equations used in this model are explained in detail in this chapter.

3.2. Adsorption in a single porous pellet

As mentioned earlier, the mass transfer stages take place in series: first convection from the bulk air to the pellet surface, and then diffusion and adsorption within the pellet. Therefore the mass flux can be written as:

$$N_A = h_m(C_b - C^*) \tag{3- 1}$$

where C^* is the gas concentration at the external surface of the pellet. In order to compute C^*, a new type of concentration in the pellets, C_{avg}, which takes into account both gas and sorbed phases, is defined:

$$Average\ concentration = \frac{Adsorbent\ mass\ in\ gas\ and\ sorbed\ phases\ within\ the\ pellet}{Volume\ of\ the\ pellet}$$

$$C_{avg} = \frac{V_p(1-\varepsilon_p)Q + V_p\varepsilon_p C_p}{V_p} = \frac{V_p(1-\varepsilon_p)KC_p + V_p\varepsilon_p C_p}{V_p} \tag{3- 2}$$

$$C_{avg} = \left[(1-\varepsilon_p)K + \varepsilon_p\right]C_p = K'C_p \tag{3- 3}$$

Thus K' can be considered as a version of the linear adsorption isotherm, which can be obtained experimentally. Safari (2011) carried out experiments in order to compute the Langmuir adsorption isotherm constants, K_L and C_{s0}, for MEK adsorption in activated carbon. The method applied in that work to measure the concentration of the sorbed phase and the equilibrium gas phase shows that this data can be used to obtain K'. In fact, K' is precisely the slope of the adsorption isotherm diagram (see Section 3.5.3). Therefore at low levels of C^*, it is written as (Xu *et al.* 2011):

$$K' = C_{s0}K_L \tag{3- 4}$$

Now the mass transfer in a single pellet is governed by the following equation:

$$\frac{\partial(K'C_p)}{\partial t} = D_e\left[\frac{1}{r^2}\frac{\partial}{\partial r}\left(r^2\frac{\partial(K'C_p)}{\partial r}\right)\right] \tag{3- 5}$$

With boundary and initial conditions:

$$\frac{\partial(K'C_p(0,t))}{\partial r} = 0 \tag{3-5-1}$$

$$h_m(C_b - C^*) = D_e\frac{\partial(K'C_p(R_p,t))}{\partial r} \tag{3-5-2}$$

$$K'C_p(r,0) = C_0 \tag{3-5-3}$$

where C_0 is the initial concentration. An analytical solution for the above equation is given by (Çengel, 2007, Xu *et al.* 2011):

$$\frac{(C_b - C_p(r,t))}{(C_b - C_0)} = \sum_{n=1}^{\infty} 4\,\frac{(sin\lambda_n - \lambda_n cos\lambda_n)}{2\lambda_n - \sin(2\lambda_n)}.exp\left(-\frac{\lambda_n^2 D_e t}{{R_p}^2}\right).\frac{sin[\lambda_n({}^{r}/_{R_p})]}{\lambda_n({}^{r}/_{R_p})} \tag{3- 6}$$

Where $\boldsymbol{\lambda_n}$ is obtained from the characteristic equation:

$$1 - \lambda_n cot\lambda_n = Bi = \frac{h_m R_p}{D_e K'} \tag{3- 7}$$

Note that, at the pellet surface, i.e. at $r = R_p$:

$$C_p(R_p, t) = C^*(t), \quad (3\text{- }8)$$

Hence

$$\frac{(C_b - C^*(t))}{(C_b - C_0)} = \sum_{n=1}^{\infty} 4 \frac{(sin\lambda_n - \lambda_n cos\lambda_n)}{2\lambda_n - \sin(2\lambda_n)} . exp\left(-\frac{\lambda_n^2 D_e t}{{R_p}^2}\right) . \frac{sin\lambda_n}{\lambda_n} \quad (3\text{- }9)$$

Where C_b is the bulk concentration and C_0 is the initial concentration (at t=0). Therefore the amount of adsorbent diffusing and being adsorbed in a time period *t* within a single pellet, *J(t)*, would be:

$$J(t) = \int_0^t 4\pi {R_p}^2 . h_m . [C_b - C^*(t)] dt \quad (3\text{- }10)$$

Inserting the expression of $C_b - C^*$ from equation (3- 9) into equation (3- 10) yields:

$$J(t) = (C_b - C_0) 4\pi {R_p}^2 h_m \int_0^t \sum_{n=1}^{\infty} 4 \exp(-\lambda_n^2 D_e t / {R_p}^2) \frac{(sin\lambda_n - \lambda_n cos\lambda_n)}{2\lambda_n - \sin(2\lambda_n)} \frac{sin\lambda_n}{\lambda_n} \, dt \quad (3\text{- }11)$$

The diffusivity within the carbon particles occurs mostly through the pores. Therefore the small portion of adsorbate that diffuses through the solid part of the adsorbent pellet can be neglected compared with the portion that diffuses through the pores. In the pores, the adsorbate molecules diffuse mostly in the gas phase, however the molecules on the surface of the pores can diffuse inside via surface diffusion. For the gas phase diffusion, the effective diffusivity (the combination of molecular and Knudsen diffusion) is obtained as explained in Chapter 2. The surface diffusivity depends on the adsorption load, thus in low bulk concentrations it is negligible. Therefore the effective diffusion coefficient can be used in this model.

3.3. Adsorption in the pellets of a packed bed

The amount of adsorption in a single pellet inside a packed bed can be obtained under some simplifying assumptions, and by applying an average condition for particles located in different

positions inside the bed. The total adsorption in the bed can then be calculated as the sum of the adsorption amounts of all particles.

The model developed here is based on discretizing the space and time in the adsorption filter, which is a common practice to solve PDEs numerically. The assumptions are also the usual ones made in developing packed beds mass transfer models, but they are applied within a different approach. Indeed one important characteristic of this model is that it substitutes algebraic mass balance equations with differential equations that are then relatively straightforward to solve, which provides a simplification in comparison with previous models.

3.4. Assumptions

The assumptions made in this model are the following:

1. The particles are identical and uniformly distributed in the bed.
2. The bed is divided into N equal sections. The length of each section is dx :

$$dx = {}^{L}/_{N} \tag{3- 12}$$

dx is small enough so as to consider the bulk concentration uniform in each section. The number of particles in each section, N_{pi}, is naturally equal to:

$$N_{pi} = {}^{N_p}/_{N} \qquad \text{where } N_p \text{ is the number of pellets in the bed.} \tag{3- 13}$$

3. The radial concentration gradient in the bed is neglected.
4. The back mixing is neglected and a plug flow is assumed; this affects the mass balance equation of each section, see Section 3.5.1.
5. The interstitial velocity, u, is the average velocity that prevails in the void space of the column, it is obtained from the superficial velocity as:

$$\text{Superficial velocity} \qquad u_s = {}^{\dot{V}}/_{A_s} \tag{3- 14}$$

Interstitial velocity $$u = {u_s}/{\varepsilon_b} \quad (3\text{- }15)$$

Where $\dot{V}$ is the volume flow rate and A_s is the cross sectional area of the bed.

6. The residence time of the gas in each section is obtained via dividing the residence time of the bed by the number of sections:

Bed residence time $$t_R = {L}/{u} \quad (3\text{- }16)$$

Sections residence time $$\Delta t = {t_R}/{N} \quad (3\text{- }17)$$

7. At time t=0 the initial concentration for all pellets in bed, C_0=0 (Fresh bed).

3.5. Model description

As mentioned before, the mass balance in this model is given by an algebraic equation which is written for each section at each time step, the time steps being equal to Δt.

3.5.1. Total adsorption in each section

Consider a given bed section i, at each time step, the bulk concentration around each particle is approximately the same (assumption 2). Thus, using equation (3- 11) and the average flow conditions for all the particles in that section, one can see that the adsorption amount of each pellet, J_i, is the same. Therefore the total adsorption amount for this section, J_{Bi}, is J_i times the number of particles in the section.

$$J_{Bi} = J_i \times N_{pi} \quad (3\text{- }18)$$

The mass balance equation for section i and time step j, can now be written as below:

$$Input\ (i,j) - adsorption\ (i,j) = output(i,j) = input(i+1, j+1)$$

$$\dot{V} \times C_{b(i,j)} \times \Delta t - J_{i,j}(\Delta t) \times N_{pi} = \dot{V} \times C_{b(i+1,j+1)} \times \Delta t \quad (3\text{- }19)$$

To compute $J_{i,j}(\Delta t)$, the bulk concentration C_b and the initial concentration C_0 should be updated at each time step. In the first section, the bulk concentration is always equal to the

inlet concentration whereas in the other sections, it starts from a value less than the inlet concentration, since some contaminant has been adsorbed in previous sections. At some point, the bulk concentration eventually reaches the inlet concentration after which it remains constant, since the previous sections are saturated and do not adsorb any more contaminant. In general, $C_{b(i,j)}$ is updated automatically as the mass balance equations are solved respectively for each section at each time step.

C_0 is obtained by the summation of the adsorption amounts of all the pellets in previous time steps. It is then divided by K', in order to convert it to gas phase concentration and subtract it from the bulk concentration.

$$C_0(i,j) = \frac{\sum_0^{j-1} J_{i,j}(\Delta t)}{V_p . K'} \qquad (3\text{- }20)$$

3.5.2. Adsorption potential of the sections:

As mentioned before, in this model the bulk concentration for each section is calculated based on the amount of adsorption in the previous section. To calculate $C_{b(i+1)}$, we compare the mass that enters section *i* to the amount of contaminant that section *i* is potentially able to adsorb, $J_i \times N_{pi}$. If the input is less than $J_i \times N_{pi}$, the outlet concentration, which is the bulk concentration for the next section, naturally equals zero. If the input is more than $J_i \times N_{pi}$, the pellets in section *i* are not able to adsorb all of the contaminant that enters the section and the outlet concentration of section *i* then equals the difference between the input and the maximal possible amount of adsorption, $J_i \times N_{pi}$. Thus as section *i* saturates along this process, J_i decreases and the outlet concentration becomes equal to the inlet concentration in the section.

3.5.3. Variation of the linear adsorption isotherm constant

As seen before, the linear adsorption isotherm constant is used in this model to compute the Biot number and the characteristic values, λ_n, as well as to update the initial concentration. Figure 3-1 shows the adsorption isotherm for the MEK adsorption experimental data (Safari, 2011).

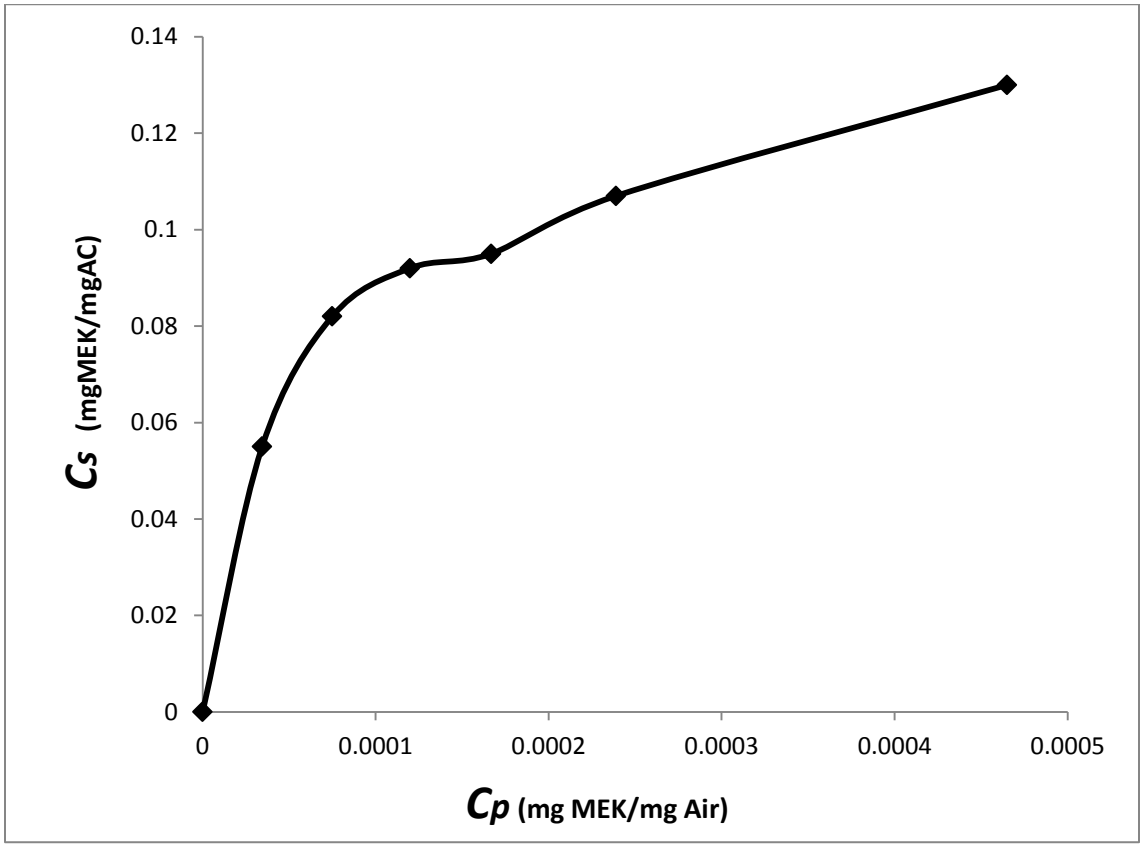

Figure 3-1: MEK adsorption isotherm

As explained before, the slope of this diagram is equal to the linear adsorption isotherm constant (K'). However this diagram shows that the slope of the adsorption isotherm curve varies with the gas concentration. At low concentration values, the slope is high and as the concentration increases the slope of the adsorption isotherm decreases. On the other hand, it is known that the bulk concentration in the bed changes from zero to the inlet concentration during the adsorption process in each section, and consequently C^* varies with the bulk

concentration. Thus it is more accurate to adjust the linear adsorption isotherm for different ranges of concentration during the process.

Comparing the linear and Langmuir adsorption isotherms, the linear adsorption isotherm can be adjusted as follows:

$$K' = \frac{C_{s0}K_L}{1 + K_L C^*} \tag{3- 21}$$

In that way K' is adjusted as the gas concentration (C^*) changes, so that when the gas concentration is low, the linear adsorption isotherm is high and as the gas concentration increases in each section during the adsorption process, K' decreases.

The effect of the variation of K' on the Biot number and on the characteristic values was studied. Table 3-1 shows that the adsorption amount, $J(t)$, does not vary significantly with the variation of the linear adsorption isotherm: the variation is less than 0.2%. For the Biot number computations, it is therefore not necessary to adjust the values of K' according to the gas concentration variations in the bed.

Table 3-1: Effect of *K* variation on characteristic values and adsorption amount

C^* *(ppm)*	$K = \frac{C_{s0}K_L}{1 + K_L C^*}$ *(m^3Air/m^3AC)*	$\int_0^{\Delta t} \sum_{n=1}^{10} 4\exp(-\lambda_n^2 D_e t/{R_p}^2) \frac{(sin\lambda_n - \lambda_n cos\lambda_n)}{2\lambda_n - \sin(2\lambda_n)} \frac{sin\lambda_n}{\lambda_n} dt$
0	2,499.97	2.380×10^{-5}
15	1,502.34	2.379×10^{-5}
30	1,030.60	2.379×10^{-5}
50	747.67	2.378×10^{-5}
70	586.62	2.377×10^{-5}
100	439.56	2.375×10^{-5}

However to calculate the initial concentration, C_0, at each time step, C_{avg} should be converted to the equilibrium gas concentration by using a value of K' in the proper range of gas concentration. Therefore the adjusted linear adsorption isotherm is used in this instance.

3.5.4. Number of characteristic values

Equation (3- 9) shows that the analytical solution of the mass transfer equation for a single particle is a function of a sum featuring an infinite number of characteristic values, but it is clear that the effect of these characteristic values decreases as their index increases. Thus the next step is to find the number of λ_n's that is needed to compute the adsorption amount, *J(t)*. It is usually estimated that for $D_e t/{R_p}^2 > 0.2$, keeping the first term λ_1 and neglecting all the remaining terms in the series results in an error that is less than 2% (Çengel, 2007). In Table 3-2 series with one and ten characteristic values are compared. Although in the experimental data used in this study, $D_e \Delta t/{R_p}^2 \not> 0.2$, the error was found to be less than 1.5% and it was finally decided to make use of only the first characteristic value, λ_1, in the model computations.

Table 3-2: Comparing the effect of the number of characteristic values on adsorption amount

K *(m^3Air/m^3AC)*	$\int_0^{\Delta t} \exp(-\lambda_1^2 D_e t/{R_p}^2)\ \frac{(sin\lambda_1 - \lambda_1 cos\lambda_1)}{2\lambda_1 - \sin(2\lambda_1)}\ \frac{sin\lambda_1}{\lambda_1}\ dt$	$\int_0^{\Delta t} \sum_{n=1}^{10} 4\ \exp(-\lambda_n^2 D_e t/{R_p}^2)\ \frac{(sin\lambda_n - \lambda_n cos\lambda_n)}{2\lambda_n - \sin(2\lambda_n)}\ \frac{sin\lambda_n}{\lambda_n}\ dt$
2,499.97	2.37421×10^{-5}	2.380×10^{-5}
1,502.34	2.36935×10^{-5}	2.379×10^{-5}
1,030.60	2.36379×10^{-5}	2.379×10^{-5}
747.67	2.35709×10^{-5}	2.378×10^{-5}
586.62	2.35039×10^{-5}	2.377×10^{-5}
439.56	2.34001×10^{-5}	2.375×10^{-5}

3.6. Model parameters

The input parameters of this model were either computed or measured in experiments which have been done for volatile organic compounds at different inlet concentrations in the indoor air quality laboratory of Concordia University. Some of these tests have been done by former students and some by a group of students including the author. There are two groups of experimental data: the small scale tests and the large scale tests. Safari (2011) and Kholafaei

(2009) described in detail the small and the large scale experimental setups, respectively. This is recalled briefly in the following.

- Small scale experimental setup: This system consists of a cylindrical packed bed filter filled with cylindrical granular activated carbon and the contaminants used in these tests are MEK and n-hexane. The sizes of the bed and particles are given in Table 3-3. The system comprises an air flow controller to adjust the air flow rate and a desiccator to dry up the air before the contaminant injection port. At the injection port, the volatile organic compound is injected via a syringe into the air with a constant injection rate, which is chosen so as to obtain the desired inlet concentration according to the air flow rate. After the injection port and before entering the filter, the upstream concentration is measured with a photo-acoustic gas detector, B&K, every 10 minutes in order to ensure a constant inlet concentration. After the filter, the downstream concentration is measured again with the second photo-acoustic gas detector, INNOVA, every 2 minutes in order to obtain the breakthrough curve of the process. The test continues until the downstream concentration reaches the upstream concentration and the filter saturates completely.
- Large scale experimental setup: In this system the filter is installed in a full scale duct. This system is more complicated than the small scale setup and it has different parts to prepare the air before entering the filter: a variable-speed blower to provide different air flow rates, high efficiency particular air (HEPA) filters to remove particulate pollutants, and a humidifier to humidify the air. This last part was used study the effect of relative humidity on the performance of the activated carbon

packed bed filter in previous studies (Khazraei *et al.* 2011). However there is no dehumidifier to dry up the air, thus experimental data in this work is selected for the case of minimum possible relative humidity, which is 25%. The experimental procedure in this system is similar to that of the small scale setup, since there is an injection port for the contaminant before the filter, and the upstream and downstream concentrations are measured in specific time periods to obtain the breakthrough curves. However the injection and concentration measurements are carried out differently. An auto-sampler device takes samples every 2 minutes from the upstream and downstream air respectively and sends them to the gas detector, INNOVA, to measure the concentrations. It should be noted that after upstream sampling the auto sampler takes some laboratory air in order to prevent the upstream perturbation on downstream results in INNOVA. In this test the contaminant is MEK. The injection procedure is also different than for the small scale test. In a full scale duct the contaminant does not inject directly by a syringe, while a bubbling system is applied to inject a single contaminant to the air in the duct. In a bubbling system the air, with a determined flow rate, basically passes the contaminant in a bottle and carries the evaporated contaminant to the injection port. To adjust the inlet concentration, the flow rate of the air should be adjusted with the air flow controller. The activated carbon used in full scale test is the same as small scale tests and the size of the filter is given in Table 3-3. The input parameters of these models are classified in the following three sections.

3.6.1. Packed- bed characteristics

The size of the bed and particles, number and density of particles, packing density and porosity of the bed are explained first.

Since the particles in a packed bed are in contact, the available surface area for mass transfer is less than the sum of the pellets external surface area. The surface area coefficient (*ω)* is a coefficient between zero and one which specifies the available surface area of the pellets in the bed. Safari (2011) defined the available surface coefficient as:

$$\omega = \frac{PD}{\rho_{AC}} \tag{3- 22}$$

ρ_{AC} is the activated carbon density and the packing density of a packed bed, *PD*, is defined as below:

$$PD = \frac{mass\ of\ adsorbent\ particles\ in\ the\ bed}{volume\ of\ the\ bed} = \frac{M_s}{V_b} \tag{3- 23}$$

Thus the available surface area of the particles, *A*, is computed as below:

$$A = \omega \times A_p \times N_p \tag{3- 24}$$

Where A_p is the external surface area of the particle. The number of particles in the bed is equal to the particles total mass divided by the mass of a single particle. If the particles in the packed bed are not spherical, the equivalent spherical diameter, d_e, should be obtained.

$$V_p = {}^{4}/_{3}\,\pi(\frac{d_e}{2})^3 \tag{3- 25}$$

One can find the bed parameters for large and small scale experiments in Table 3-3.

Table 3-3: Packed-bed characteristics

Parameter	Small scale test	Large scale test
Bed diameter, length (cm)	5.08, 3	58.42×58.42× 5.08
Particle diameter, length (mm)	2.5, 6	2.5, 6
Equivalent spherical diameter for particles(mm)	3.82	3.82
Mass of activated carbon particles in the bed(mg)	25000	7.52×10^{6}
Mass of one particle (mg)	23	23
Density of activated carbon (kg/m^3)	450	450
Packing density (kg/m^3)	411.2	433.7
Surface area coefficient	0.9	0.96
Number of particles in the bed	1,087	326,956
Bed void	0.47	0.44

3.6.2. Air flow conditions

Flow conditions such as the volume flow rate and the MEK inlet concentration in the tests are adjusted during the process. Other parameters can then be computed from these data. The flow parameters are tabulated in Table 3-4.

Table 3-4: Flow conditions in experimental setups

Flow parameters	Small scale test	Large scale test
Air flow rate (lit/min)	30	13,140
Superficial air velocity (m/min)	14.8	38.5
Air velocity inside the bed (m/min)	31.49	87.5
Residence time in the bed(min)	9.5×10^{-4}	5.8×10^{-4}
Air temperature (K)	296±1	296±1
Relative humidity (%)	0	25

Small scale tests have been done for MEK with different inlet concentrations: 15, 30, 50, 70, 100, 200 ppm

Large scale tests have been done for MEK with inlet concentration of 18ppm

3.6.3. Mass transfer coefficients and adsorption isotherm parameters

The last group of model input parameters are the physical characteristics of air, the adsorption isotherm constants of the VOCs-Air-Activated Carbon system and the bed mass

transfer coefficients, see Table 3-5. It should be noted that some physical properties of MEK and n-hexane are very similar, such as diffusivities.

The adsorption isotherm parameters used to compute the linear adsorption isotherm at each step are derived from laboratory experiments (Safari 2011). Since these constants were obtained in mass units (mg/mg), the units of concentrations used in this model were changed for mass units (mg/mg). The convective mass transfer coefficient for particles in the packed bed, h_m, is obtained from the Wakao-Funazkri correlation presented in Chapter 2. Dimensionless numbers that are applied in this correlation are presented in Table3-6.

Table 3-5: Physical properties of the adsorbate-adsorbent system

Parameters for VOC-Air-Activated Carbon system	Small scale test	Large scale test
Air density (kg/m^3)	1.204	1.204
Air kinematic viscosity (m^2/s)	1.5×10^{-5}	1.5×10^{-5}
K_L (mgAir/mgVOC) for MEK	19531	19531
C_{s0} (mgVOC/mgAC) for MEK	0.128	0.128
K_L (mgAir/mgVOC) for n-hexane	7407	-
C_{s0} (mgVOC/mgAC) for n-hexane	0.272	-
MEK/n-hexane molecular diffusivity (m^2/s)	8×10^{-6}	8×10^{-6}
MEK/n-hexane convective mass transfer coefficient (m/s)	0.04	0.065
MEK/n-hexane effective diffusivity (m^2/s)	2×10^{-6}	2×10^{-6}

Table 3-6: Dimensionless numbers

Non-dimensional Number	Small scale test	Large scale test
Re	62.81	162.98
Sc	1.83	1.83
Sh	18.13	30.53

Chapter 4: Results and discussion

4.1. Model development

The model proposed here is implemented with MATLAB. There are two options in writing and solving the mass balance equations for the sections of the bed during the adsorption time steps until bed saturation. The first is to solve the mass transfer equations in the first section (whose inlet concentration is given) for every time step until the section saturates and then to use its outlet data for the second section, and so on for the next sections. The second option, which is chosen in this work, is to solve the mass balance for all the sections consecutively during the bed residence time, repeating this process for the next time steps until all sections saturate.

To validate the model, input parameters corresponding to experimental conditions are used in this model, for experiments consisting of both small scale and large scale tests of MEK adsorption in granular activated carbon packed bed filters (Table 3-3, 3-4, 3-5). The breakthrough curves for different levels of inlet concentrations (15ppm, 50ppm, 100ppm) are then plotted to be compared with the experimental data. In addition, breakthrough curves were obtained and compared with small scale experimental data of n-hexane adsorption at 30ppm, 60ppm, 100ppm inlet concentration. This approach to validating the model is standard and was developed by Safari (2011).

Furthermore, the results of the model are compared to two other popular models to show the contribution of this study. Finally, a parametric study is carried out to investigate the effect of varying certain important parameters in packed bed adsorption systems, with a specific method designed to avoid conflicts between the effects of different parameters.

4.2. Convergence study

To choose an appropriate number of sections, a convergence study is needed. Assumption 2 in Section 3.4 was that the length of the sections is small enough so as to consider the concentration is uniform in each section. This assumption is satisfied by choosing a large number of sections. However beyond a certain number of sections the breakthrough curve does not change significantly: in other words, the results converge. Figure 4-1 shows the breakthrough curves of small scale conditions for different numbers of sections. There one can see that for $N > 20$, the results converge. On the other hand, increasing the number of sections prolongs the process time of the model. This process time for different numbers of sections is given in Table 4-1. In conclusion, the convergence study is a determination of the optimal number of sections considering both the convergence and process time of the model.

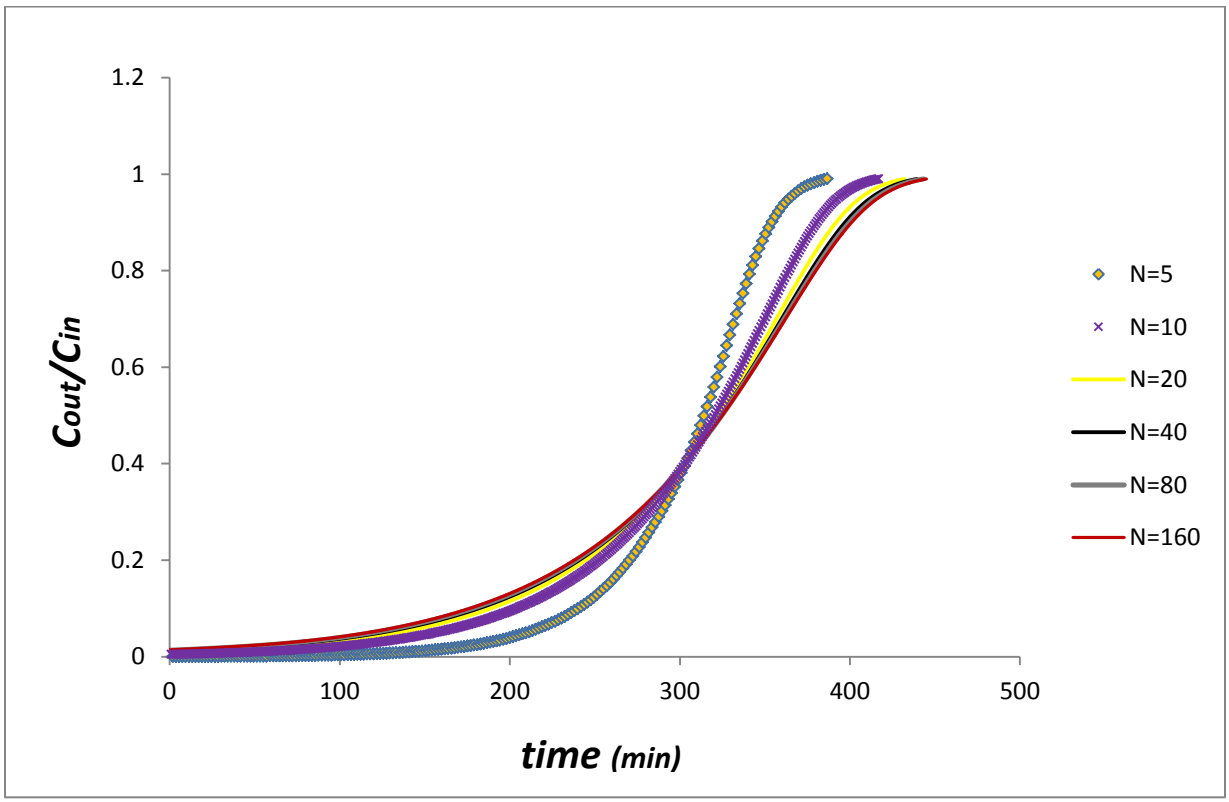

Figure 4-1: Breakthrough curves at 100ppm MEK inlet concentration, for various numbers of sections

Considering the convergence of breakthrough curves and the process time of the model, 40 sections seems an appropriate number to use in the model.

The number of sections for which convergence occurs depends on the bed characteristics and flow conditions and not on the inlet concentration. Besides, the process time of the model increases for a fixed number of sections when the inlet concentration decreases. In this work *N=40* is selected for all the inlet concentrations of small scale tests.

Table 4- 1: Process time of the implementation of the model for different numbers of sections

Number of sections	Process time (min)
5	0.44
10	1.14
20	3
40	11
80	33
160	124

4.3. Model results for small scale tests

As mentioned before, the small scale tests were done for different levels of inlet concentrations. In this work three such levels are selected to make comparisons with the prediction of the model, in order to understand the effect of the inlet concentration and to determine for which ranges of concentration the proposed model yields better results. In Chapter 3 the small scale experimental setup is explained briefly and the input parameters of the model are presented. The reader may find more details about conditions and instructions of the experiments in the previous study (Safari, 2011). While the implementation of the model stops in all cases whenever the breakthrough curve reaches 0.99, the experimental data presented here is given for until the end of the experiment at which point, for some levels of concentration, the breakthrough curve exceeds one, due to the desorption of contaminant from the particles to the air.

4.3.1. Low level of inlet concentration

Adsorption of MEK: The first group of results is obtained for adsorption of MEK at 15ppm inlet concentration. As Figure 4-2 shows, the results of the model fit very well with the experimental data. The curve of results of the model is above that of the experiment before the 70% breakthrough and is below after it, which is reflected in the sign of the errors.

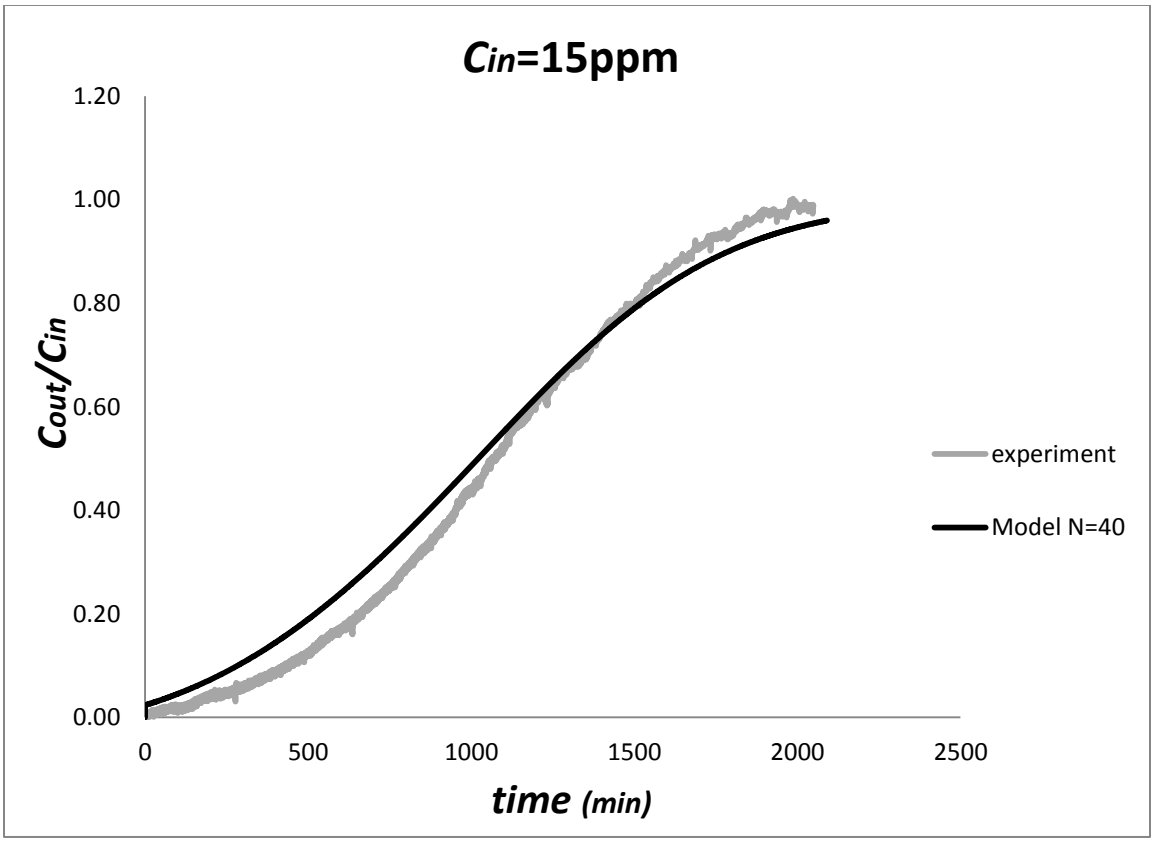

Figure 4-2: Comparison of model results and the experiment, at 15ppm MEK inlet concentration

The errors of this model for a 15ppm inlet concentration and for 20%, 50% and 80% breakthrough are shown in Table 4-2. The minimum error is between 60-80% breakthrough and the error increases again after that until the saturation point.

Table 4-2: Error of the proposed model at 15ppm MEK inlet concentration

Breakthrough	Time(min) model	Time(min) experiment	Error (%)
20%	521.55	667.52	21.87
50%	1021.20	1063.15	3.95
80%	1520.60	1502.95	-1.17

Adsorption of n-hexane: The breakthrough curve of n-hexane for 30ppm inlet concentration is obtained and shows a good agreement with experiments (Figure 4-3).

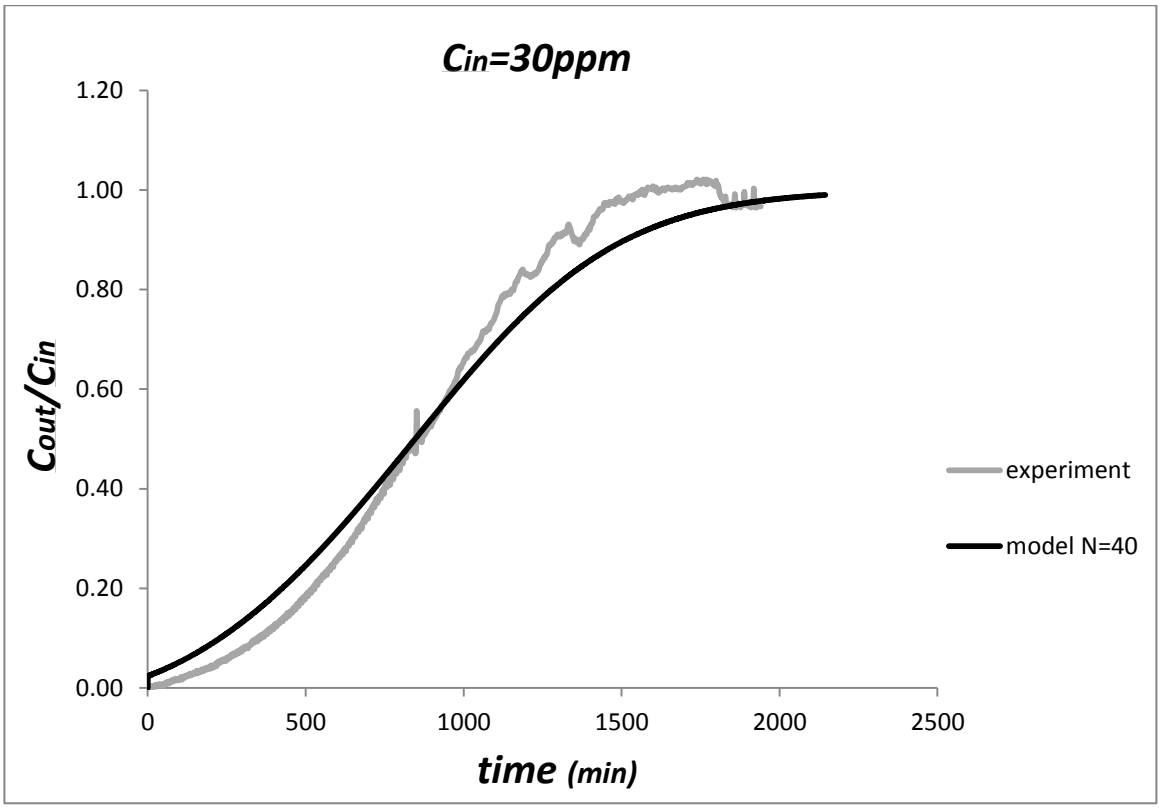

Figure 4-3: Comparison of model results and the experiment, at 30ppm n-hexane inlet concentration

It is important to mention here that the convergence study was also done for n-hexane and that based on that study the number of sections N=40 was found to be appropriate again.

4.3.2. Middle level of inlet concentration

Adsorption of MEK: For middle level of inlet concentration the breakthrough curve is obtained for adsorption of MEK at 50ppm inlet concentration. At this level of concentration,

the test was done twice with the same conditions in order to verify the repeatability of the experiment. Figure 4-4 shows a good fit of the model results with the experimental data.

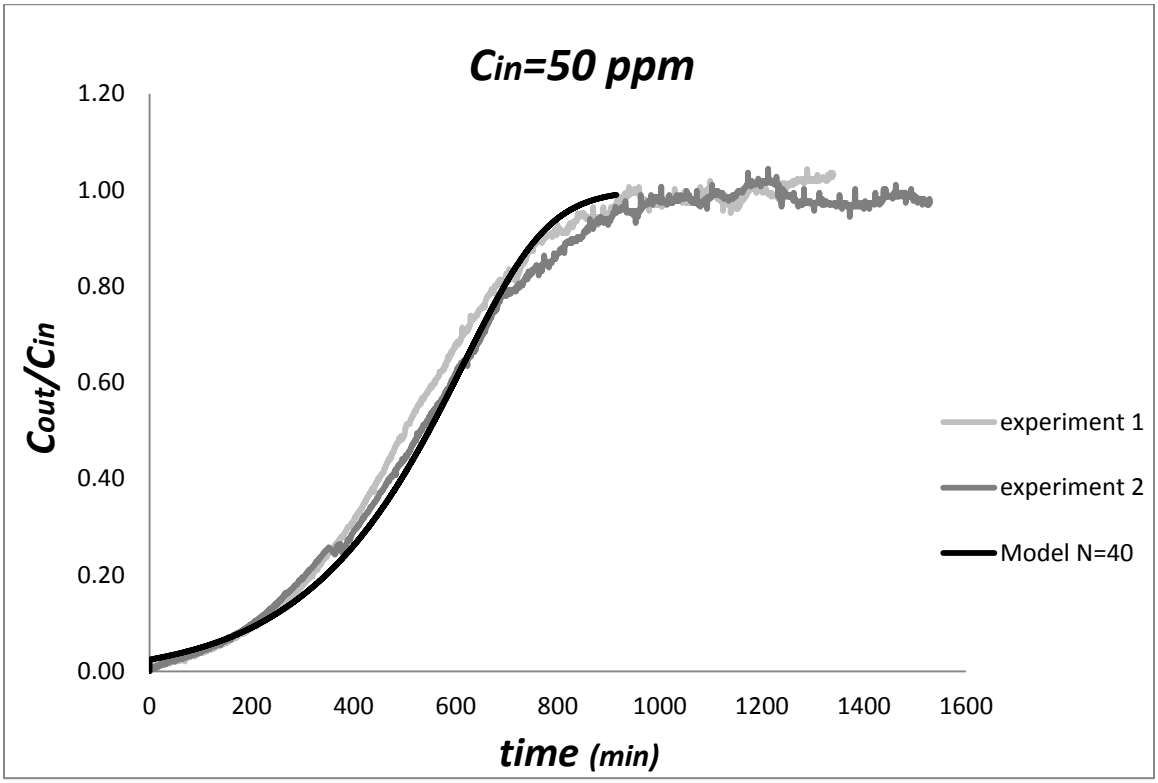

Figure 4-4: Comparison of model results and the experiment, at 50ppm MEK inlet concentration

Adsorption of n-hexane: The breakthrough curve of n-hexane at 60ppm inlet concentration (middle level) is obtained and again shows a good agreement with experiments (Figure 4-5).

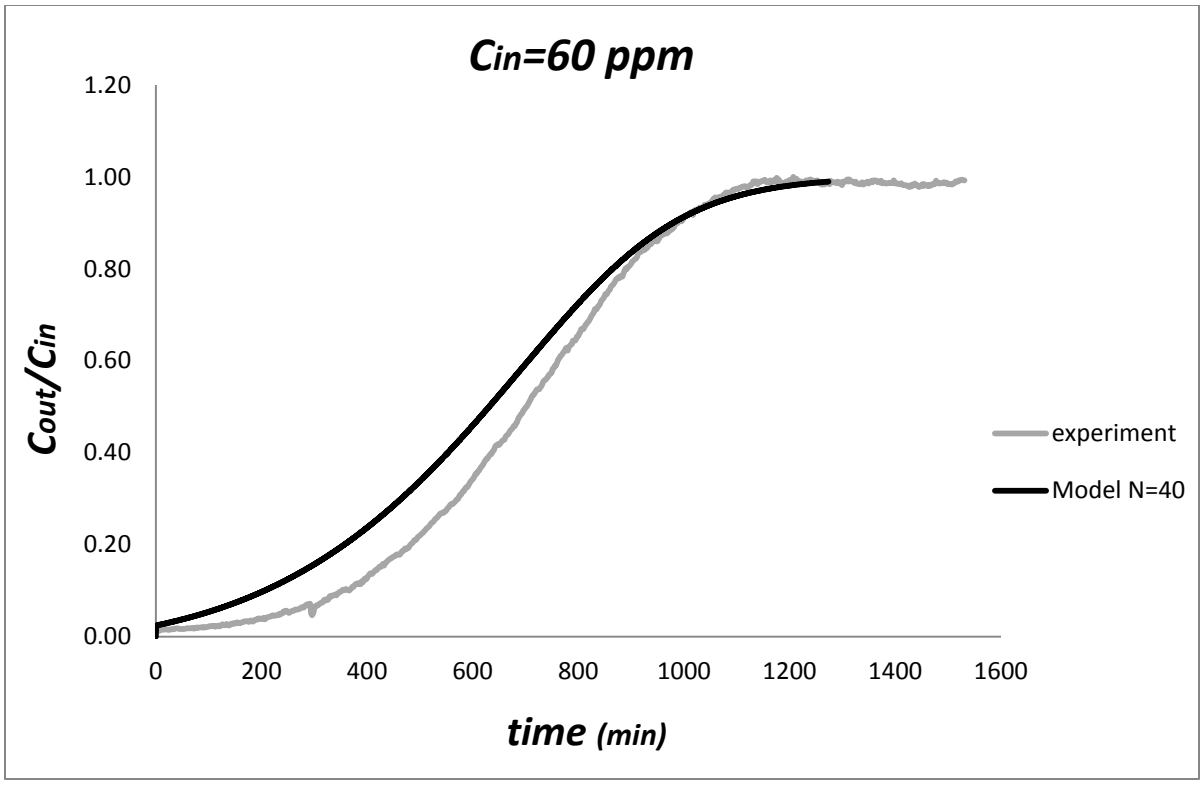

Figure 4-5: Comparison of model results and the experiment, at 60ppm n-hexane inlet concentration

4.3.3. High level of inlet concentration

Adsorption of MEK: This group of results corresponds to 100ppm inlet concentration for MEK. Figure 4-6 shows some discrepancy for high levels of MEK inlet concentration.

Adsorption of n-hexane: The results of the model for n-hexane adsorption at 100ppm inlet concentration are compared with the experimental data in Figure 4-7. Unlike in the MEK case, the results fit well with the experiments.

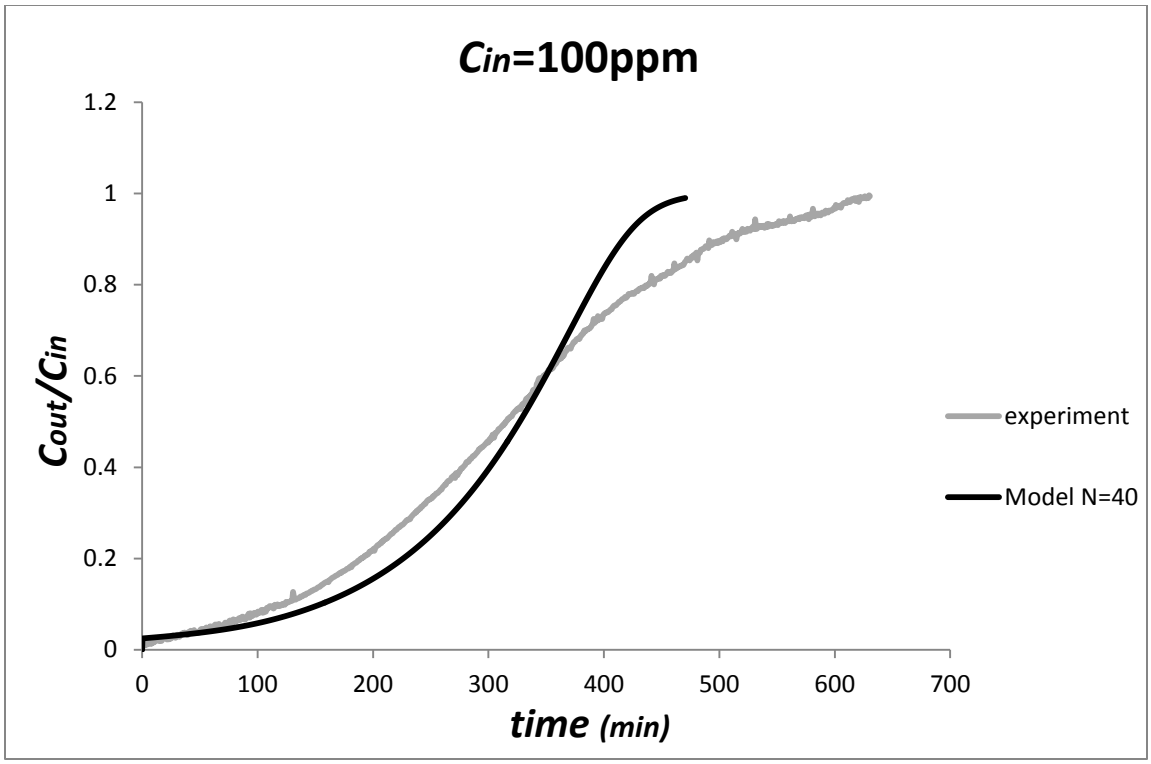

Figure 4-6: Comparison of model results and the experiment, at 100ppm MEK inlet concentration

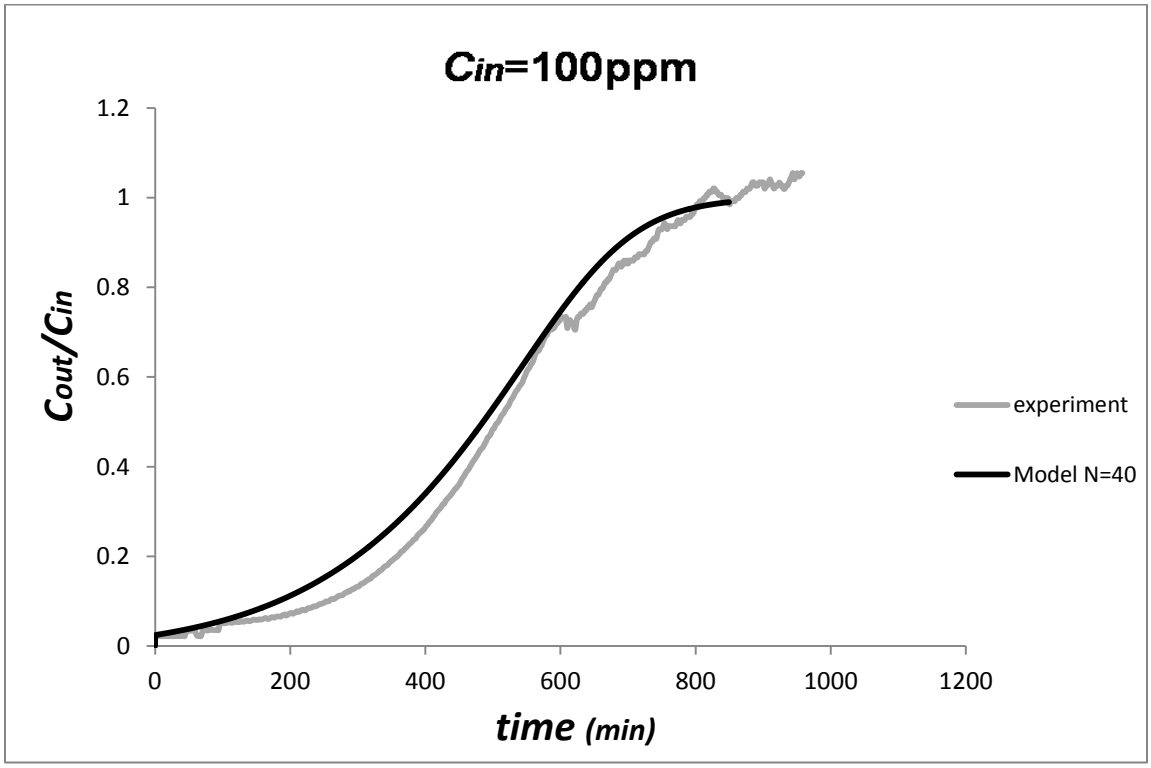

Figure 4-7: Comparison of model results and the experiment, at 100ppm n-hexane inlet concentration

Since the error in high concentration ranges of MEK is not observed for high levels of n-hexane concentration, the source of error might be related to different properties of MEK and n-hexane. The first guess was that because of different trends of the adsorption isotherm of MEK and n-hexane, for high levels of MEK concentration the use of a constant adsorption isotherm coefficient, K, as explained in Section 3.5, to calculate the characteristic values, may result in some error. To evaluate this guess, the model was modified to adjust K for different levels of bulk concentration during the adsorption process in the hope that it yields better results. However the results obtained were almost the same and further the process time of the model grew longer. This seems to indicate that the problem is not due to the adsorption isotherm constant.

Safari (2011) has compared the physical properties of these two compounds (Table 4-3).

Table 4-3: Physical properties of n-hexane and MEK

Chemical Category	Chemical Name	Molecular Formula	M.W	BP (˚C)	VP at 20℃ (mmHg)	Solubility in water at 20℃ (g/l)	Polarity
Alcane	n-hexane	C_6H_{14}	86.2	69	132	Insolubale	Non-polar
Ketone	MEK	C_4H_8O	72.1	80	78	290	Polar

There may be factors or parameters that affect the adsorption of MEK in high concentration levels whose effect does not appear in the adsorption isotherm parameters.

In summary, the model can predict the performance of GAC packed bed filters in small scales for low and middle ranges of concentrations. For high levels of concentration the error in MEK case first brought up a possible defect of the model, however running the model for another compound in the same range of concentration was successful. Thus other parameters or factors may have to be considered for adsorption of certain compounds in packed beds.

4.4. Model results for large scale tests

The large scale tests parameters are given in Chapter 3. Kholafaei (2009) explained the experimental setup. Different methods to inject the contaminants in the duct were also described in that work. Here the same experimental setup is used. The cross sectional area of the filters for large scale tests is square, and the size of the square is given in Table 3-3. A bubbling generation system was used to inject the single gas, MEK, into the duct. Although the generation system was adjusted to keep the inlet concentration of MEK constant at 20ppm, the average amount of inlet concentration at the end of the test was found to be 18ppm. Indeed fluctuations are unavoidable because, given the large size of the setup, controlling the test conditions is more difficult than for small scale tests. Another difference between conditions in small and large scale tests is that, in large scale tests, it is not possible to dry up the air. Therefore the experimental data used here corresponds to the minimum range of relative humidity for large scale tests, that is 25%. The auto sampler device was used to conduct the samples of inlet air, lab air and outlet air respectively to a photo-acoustic gas detector, INNOVA, in order to measure their concentration.

Figure 4-8 shows a comparison of the results of the model with the experimental data for large scale tests. Another convergence study showed that a number of 40 sections is again appropriate.

Since there are some fluctuations in the experimental data, a trend line is fitted to the experimental curve to be able to compare the results better. The model seems to predict the performance of the large scale filter well.

Finally, errors between the time predicted by the model and the one shown by experimental data at 50% breakthrough ratio, for all these seven comparison cases, are presented in Table 4-4.

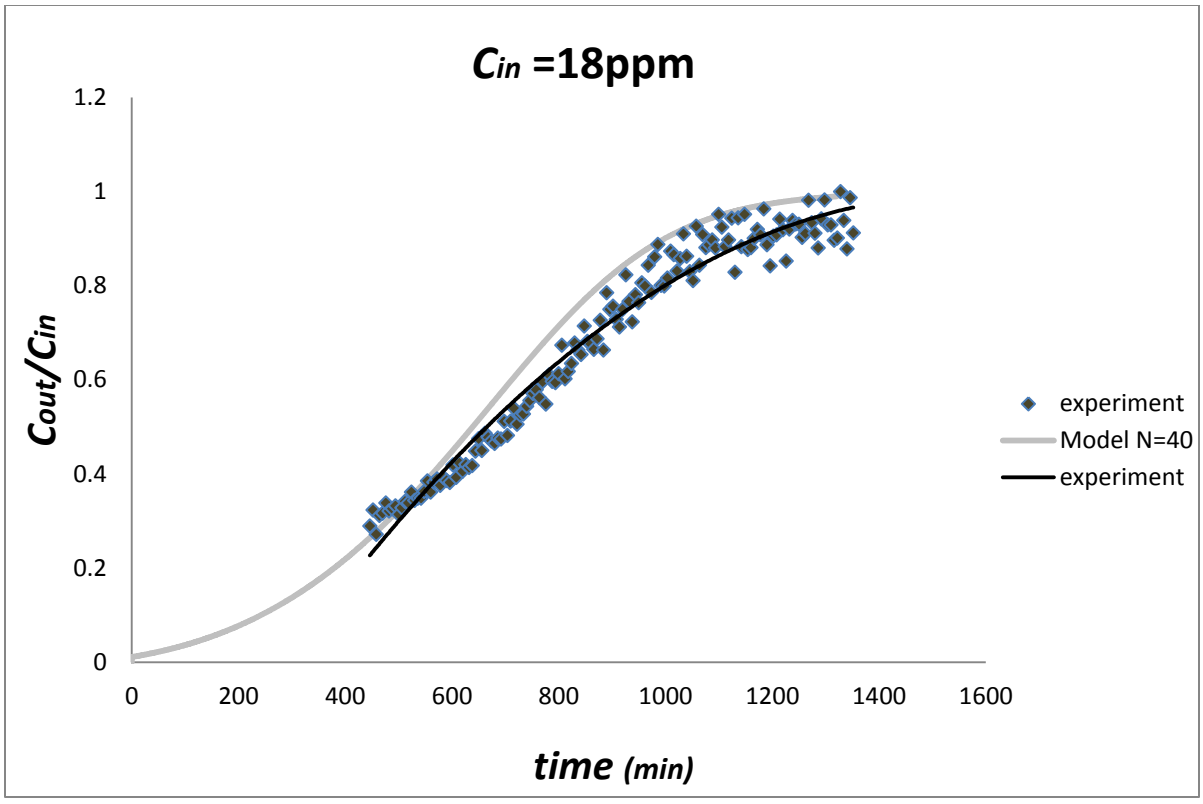

Figure 4-8: Comparison of model results and the large scale experiment, at 18ppm MEK inlet concentration

Table 4-4: Error at 50% breakthrough ratio between model prediction and experimental data

Experimental setup/Component/Concentration	Error at 50% breakthrough ratio (%)
Small scale/ MEK/ 15ppm	3.95
Small scale/ MEK/50ppm	2.4
Small scale/ MEK/100ppm	0.3
Small scale/ n-hexane/30ppm	0.8
Small scale/ n-hexane/60ppm	8.9
Small scale/ n-hexane/100ppm	0.2
Large scale/ MEK/18ppm	8.2

4.5. Model intercomparison

In this section, the results of two models previously introduced and explained in Chapter 2 are presented for comparison with the proposed model. One of these models is the analytical

solution of Rosen and the second one is the numerical model of Popescu et al. (2007). Both of these models are representative of packed bed performance modeling: similar assumptions or methods have been applied in other studies. They were both implemented for small scale experiments of MEK and n-hexane adsorption and for two different levels of inlet concentration to obtain the breakthrough curve of the packed bed during the adsorption process.

As mentioned before, in the Rosen model the linear adsorption isotherm is applied, and in this section it is considered to be equal to $K_L \cdot C_{s0}$. To calculate the infinite integrals arising in equation (2-59), a numerical integration code was written in MATLAB using the standard method of discretizing the area below the diagram according to the rectangle rule.

The Popescu model was made available for the author to get results from and Safari (2011) has applied this model for certain high levels of inlet concentration in her work.

4.5.1. The Rosen model

One important point about this analytical solution is that the final answer for the breakthrough does not depend on the inlet concentration. In other words, there is no input parameter corresponding to the inlet concentration in the infinite integrals and therefore the results for all the concentrations are the same for a fixed set of bed conditions. The results of the Rosen model in Figure 4-9 predict that the packed bed of the small scale tests, at any inlet concentration of MEK, reaches the saturation time after 3000 minutes.

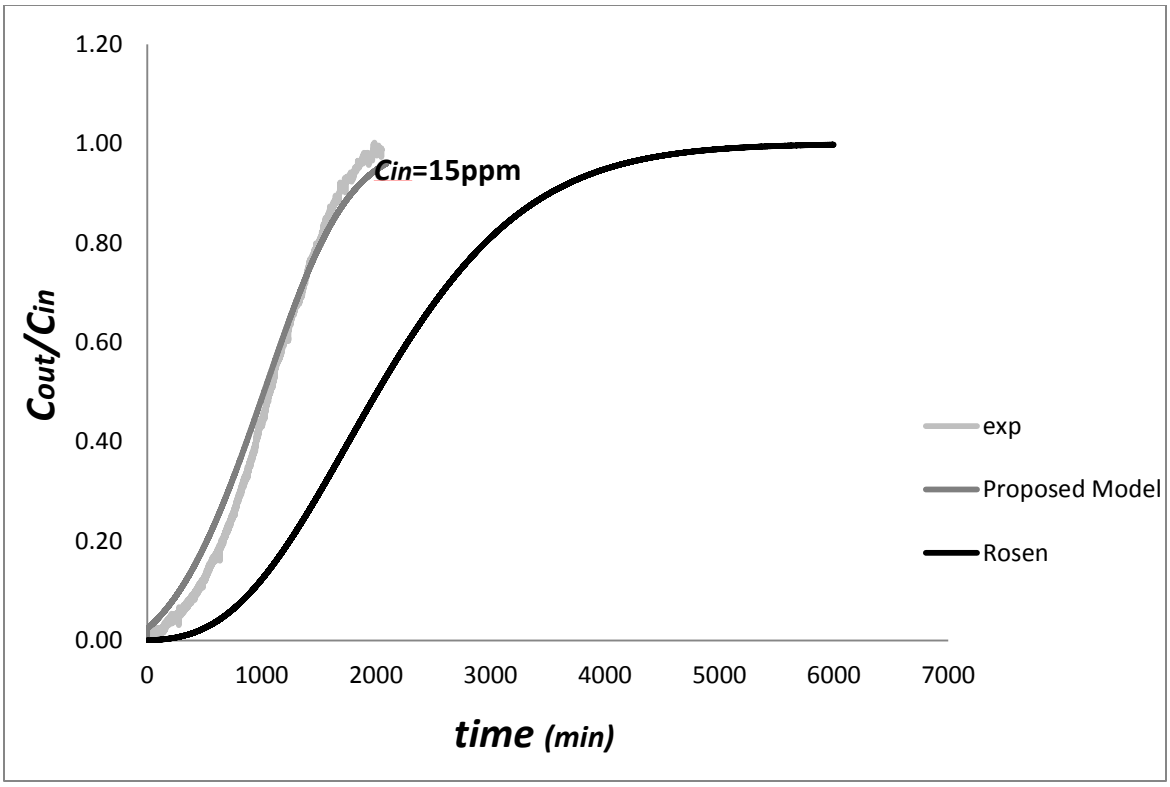

Figure 4-9: Results of the Rosen analytical solution for MEK small scale tests and comparison with the model results at 15ppm inlet concentration

The same is observed for n-hexane small scale tests: Figure 4-10 shows disagreement between Rosen model and experiments. These results conflict with the physical reality and the experimental data. Indeed the saturation time of the bed increases when the inlet concentration decreases and the experimental breakthrough curves reach the saturation point much earlier than predicted by the Rosen model, even for low levels of inlet concentrations.

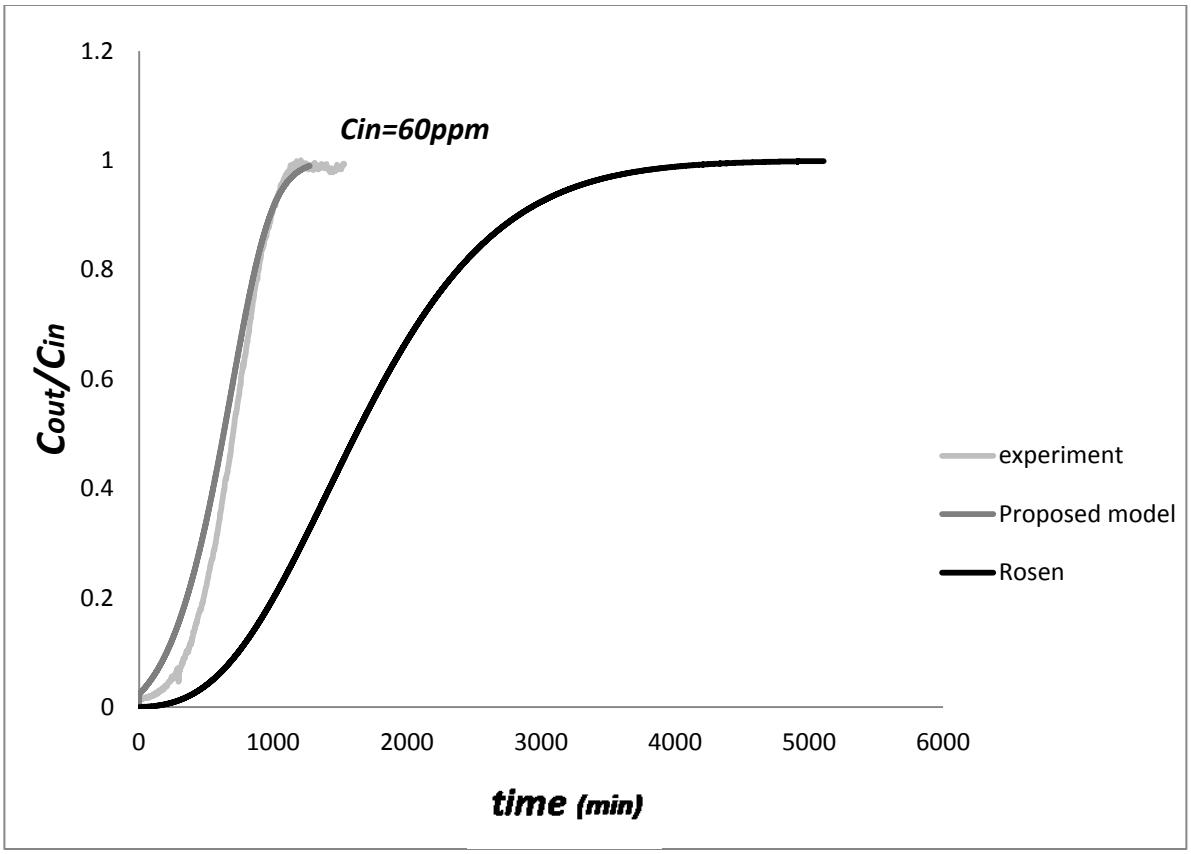

Figure 4-10: Results of the Rosen analytical solution for n-hexane small scale tests and comparison with the model results at 60ppm inlet concentration

4.5.2. The Popescu model

In this section the results of the proposed model for small scale tests at two levels of MEK and n-hexane inlet concentration are compared with the results of the Popescu model. Before presenting the comparison diagrams, a convergence study for the Popescu model is carried out in order to choose a proper number of sections. As seen in Figure 4-11 and Figure 4-12, the Popescu model converges for a number of sections larger than 10. It should be noted that although in MEK case the results show a good agreement with the experiment for $N=1$, this is not correct since the model does not converge for $N < 10$.

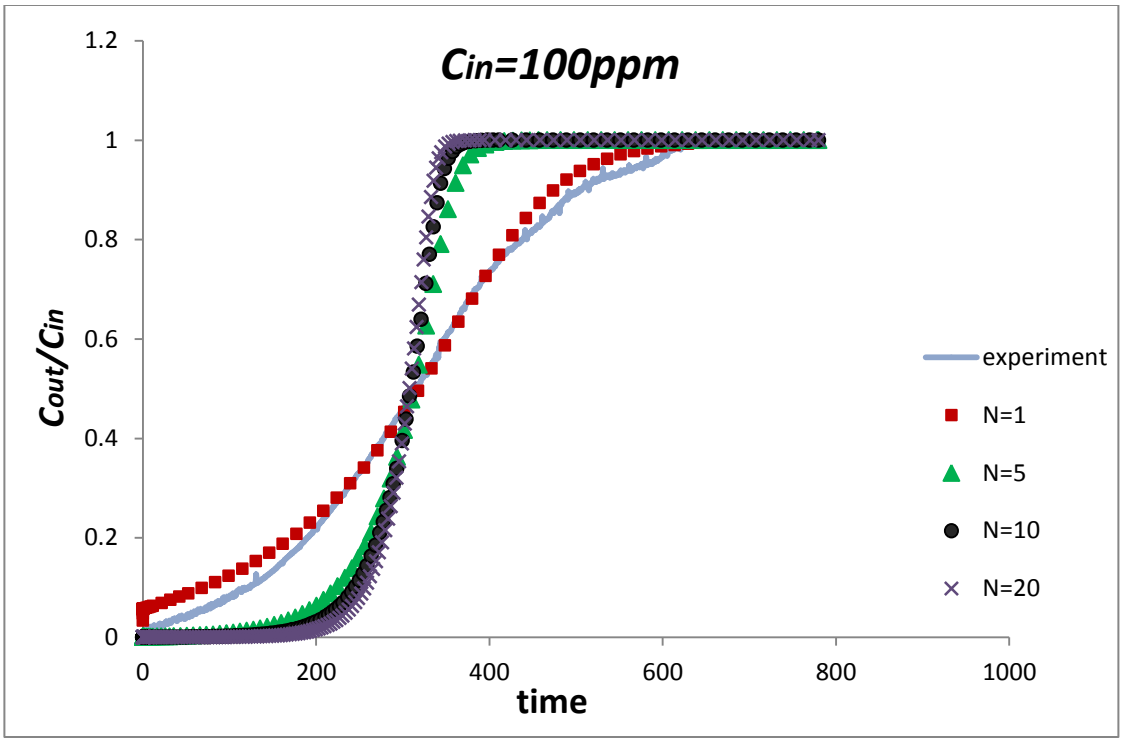

Figure 4-11: Convergence study for Popescu model for small scale test at 100ppm MEK inlet concentration

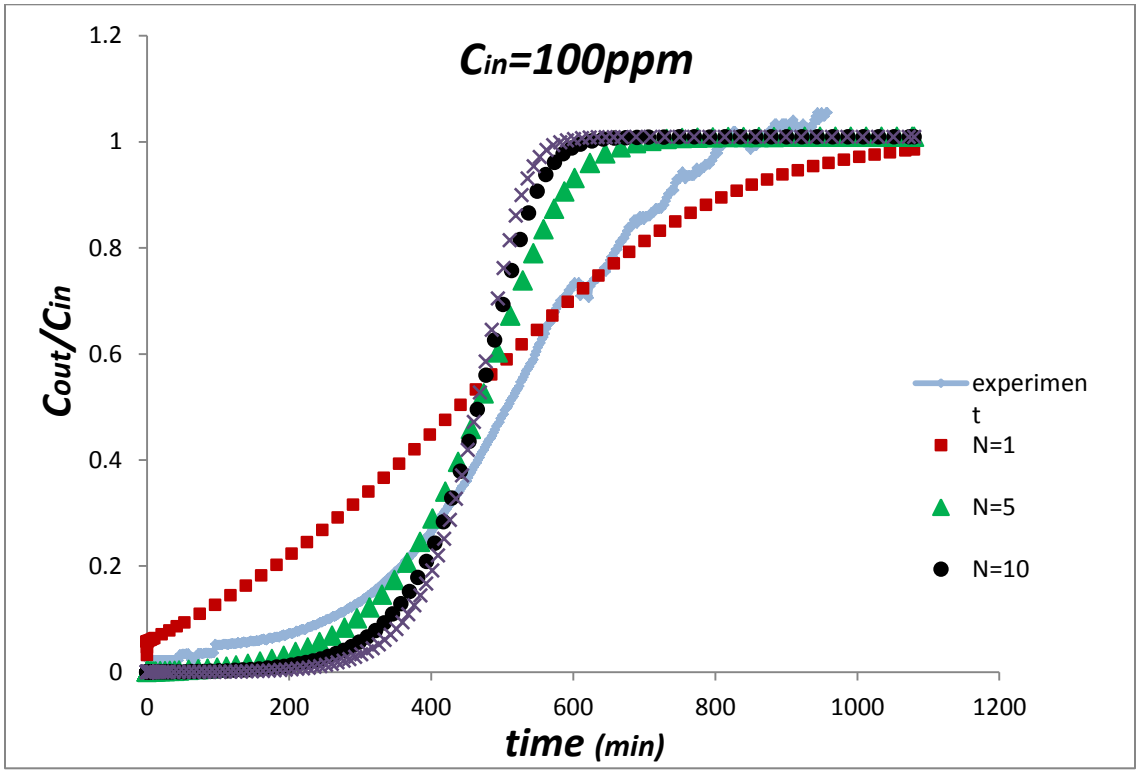

Figure 4-12: Convergence study for the Popescu model for small scale test at 100ppm n-hexane inlet concentration

In Figure 4-13 and Figure 4-14 the proposed model is compared with the Popescu model for low and middle levels of MEK inlet concentration. As these figures show that the proposed model predicts the breakthrough curve better than the Popescu model.

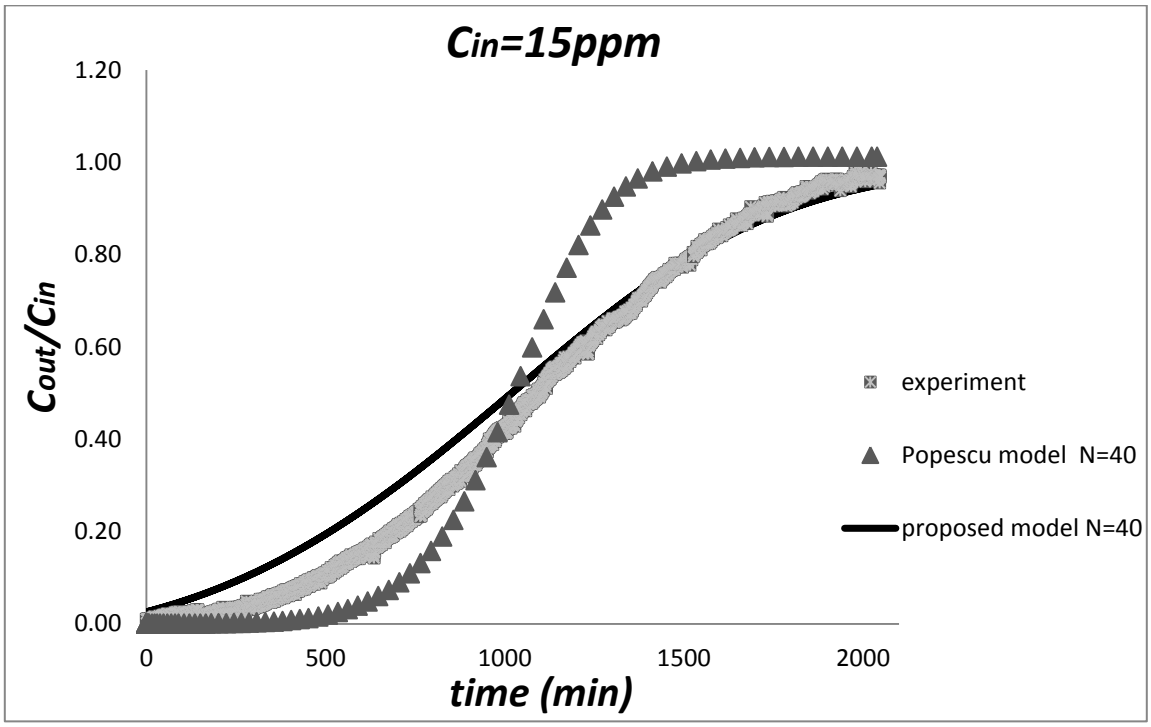

Figure 4-13: Comparison between the Popescu model and the proposed model at 15ppm MEK inlet con centration

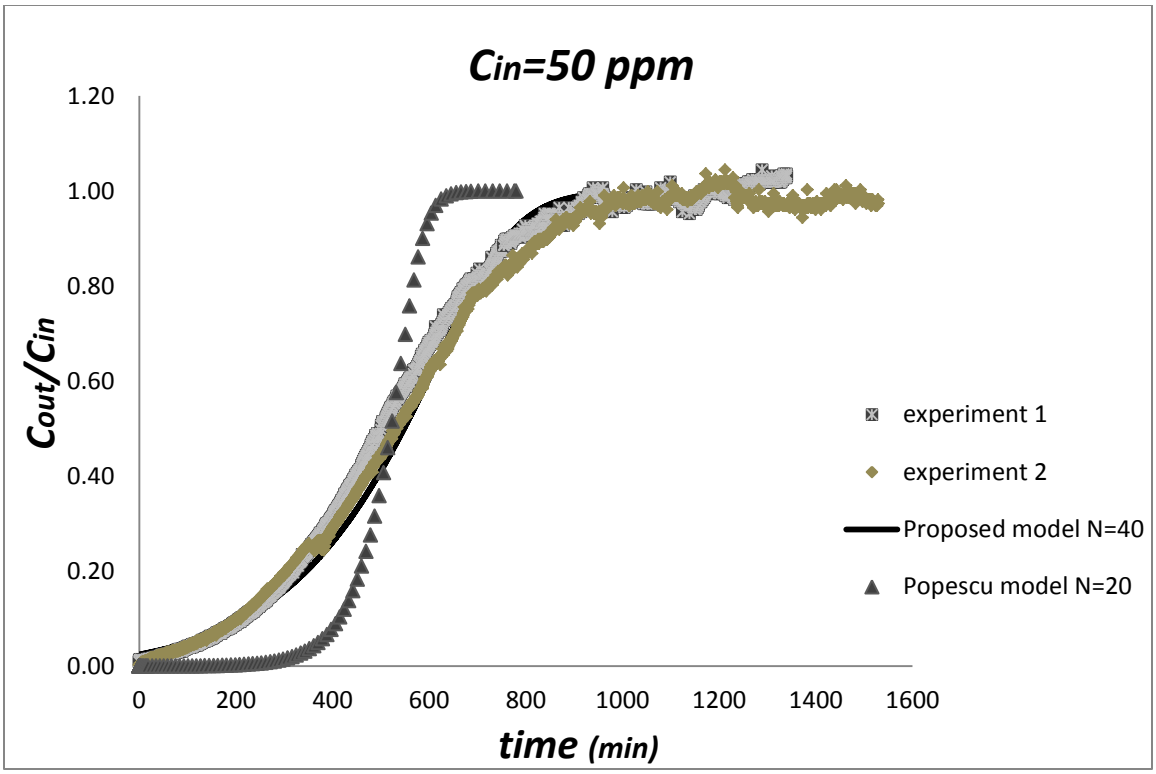

Figure 4-14: Comparison between the Popescu model and the proposed model at 50ppm MEK inlet concentration

In Figure 4-15 and Figure 4-16 the proposed model is compared with the Popescu model for low and high levels of n-hexane inlet concentration. The results of the proposed model again show a better agreement with the experiment than those of the Popescu model.

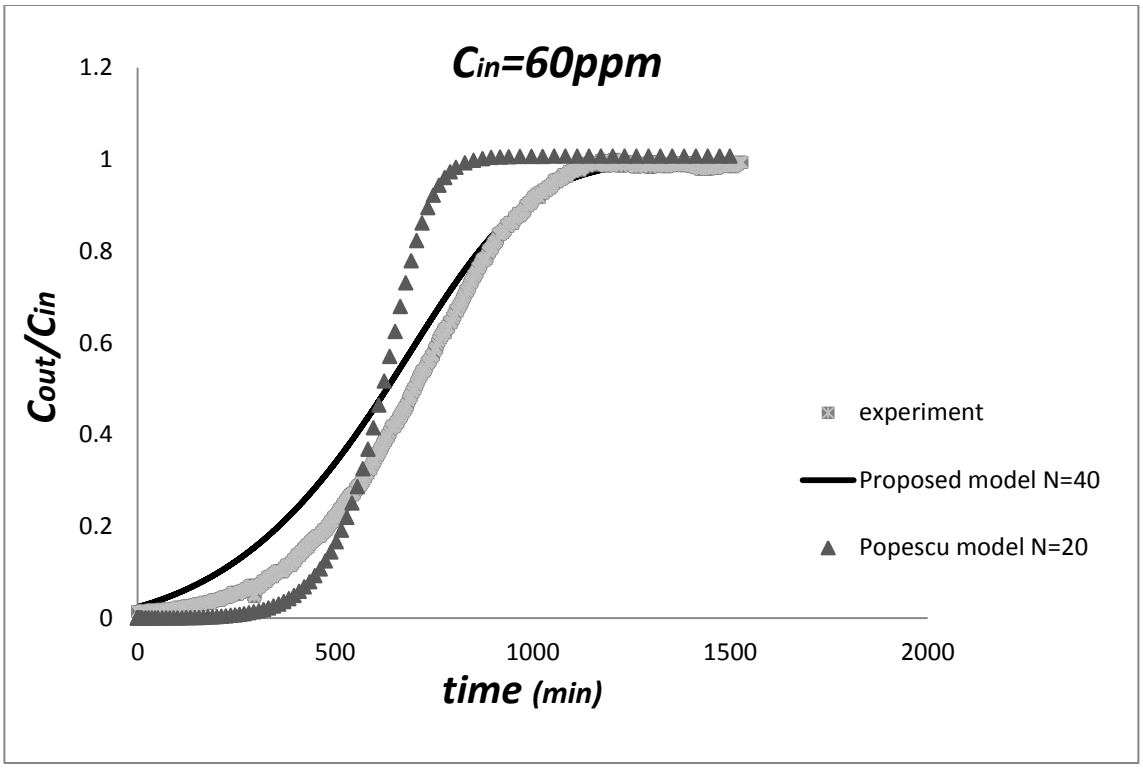

Figure 4-15: Comparison between the Popescu model and the proposed model at 60ppm n-hexane inlet concentration

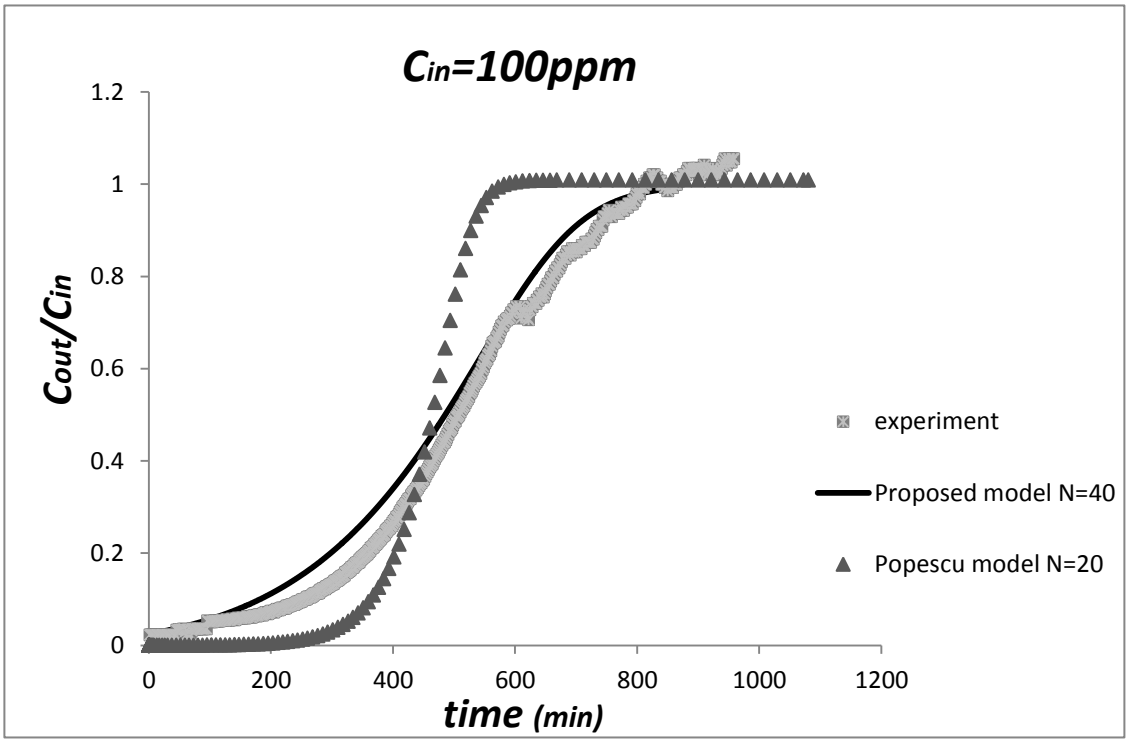

Figure 4-16: Comparison between the Popescu model and the proposed model at 100ppm n-hexane inlet cocnentration

4.6. Parametric study

Since the proposed model has been validated with the standard approach, it can be used to study the effect of different parameters on adsorption in packed beds. When studying the effect of each parameter, the other parameters should usually be kept constant so that they do not affect the results. However, as seen in Chapter 3, the input parameters of the model are related to each other and it is neither correct nor practical to vary only one parameter while keeping the others constant. For example, varying the volume flow rate (fluid velocity) affects the value of the convective mass transfer coefficient: indeed this coefficient is obtained from the Wakao & Funazkri correlation and therefore depends on the Reynolds number, and thus on the fluid velocity. Therefore a specific method is developed in order to determine the cases of the parametric study.

The non-dimensional numbers are helpful to determine in which ranges the input parameters do or do not have a significant effect on the results. For example, for large values of the Biot number the value of the convective mass transfer coefficient h_m should not affect the results, since the controlling factor is the diffusivity within the particle. Therefore the effect of the volume flow rate should be studied for large values of the Biot number in order to avoid any perturbation by the convective mass transfer coefficient.

In this section it is studied what the effect is, of changing four main operation parameters: the convective mass transfer coefficient, the diffusion coefficient within the pellets, the volume flow rate and the size of the particles.

All the parametric studies are implemented for small scale tests at 50ppm inlet concentration of MEK.

4.6.1. Convective mass transfer coefficient

In this subsection the effect of changing the value of the convective mass transfer coefficient is studied for two ranges of the Biot number in order to ensure that for high ranges of this number, the effect of this coefficient can be neglected. It should be noted that to obtain different values of h_m at fixed volume flow rate, various values of the Schmidt number are considered.

- Large Biot number (Biot >1):

  Figure 4-17 shows the results of the proposed model for different values of the convective mass transfer coefficient when the bed and flow input parameters are fixed and the diffusivity within the particles is equal to 2×10^{-8} m^2/s.

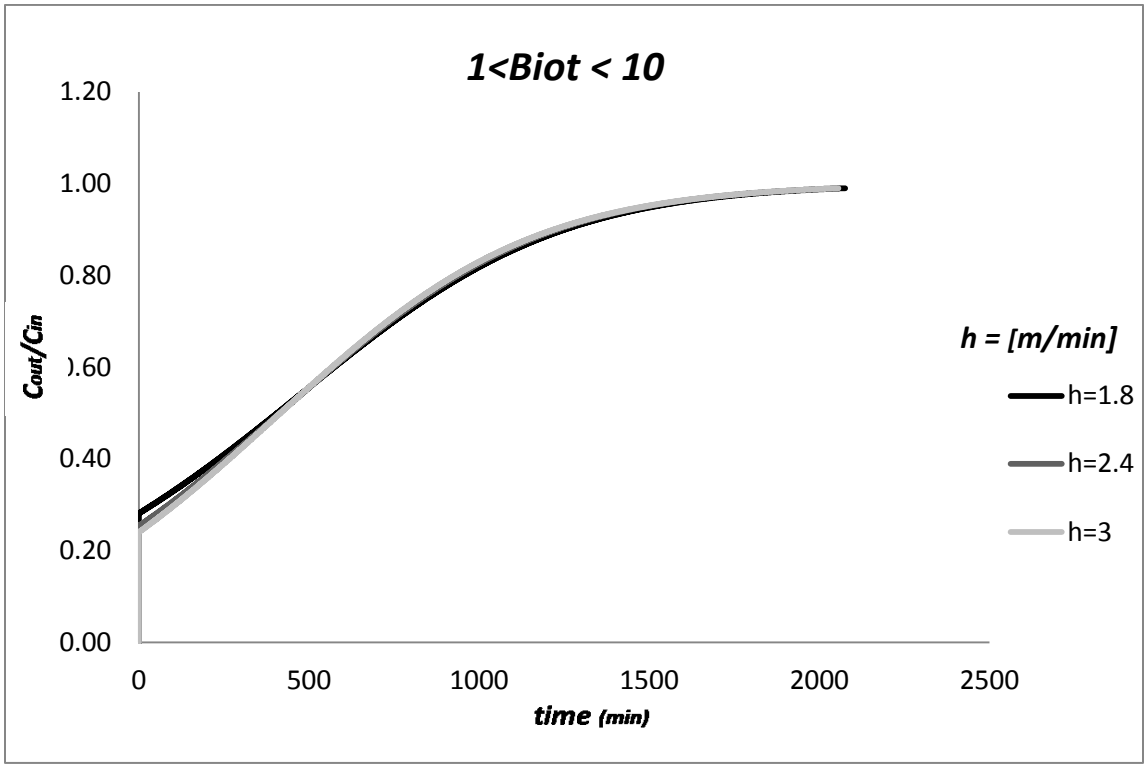

Figure 4-17: Effect of varying the convective mass transfer coefficient for large Biot number

As the figure shows, the value of the convective mass transfer coefficient does not have a significant effect on the results for large amounts of the Biot number. Indeed, as explained before, a large value of the Biot number means that the convective mass transfer resistance is much smaller than the diffusion resistance within the particles, and therefore that this term is not the controlling term for the process.

- Small Biot number (Biot < 0.1):

  Figure 4-18 shows the results of the proposed model for different values of the convective mass transfer coefficient, for small values of Biot number. The bed and flow input parameters are fixed and the diffusivity within the particles is equal to 2×10^{-6} m^2/s.

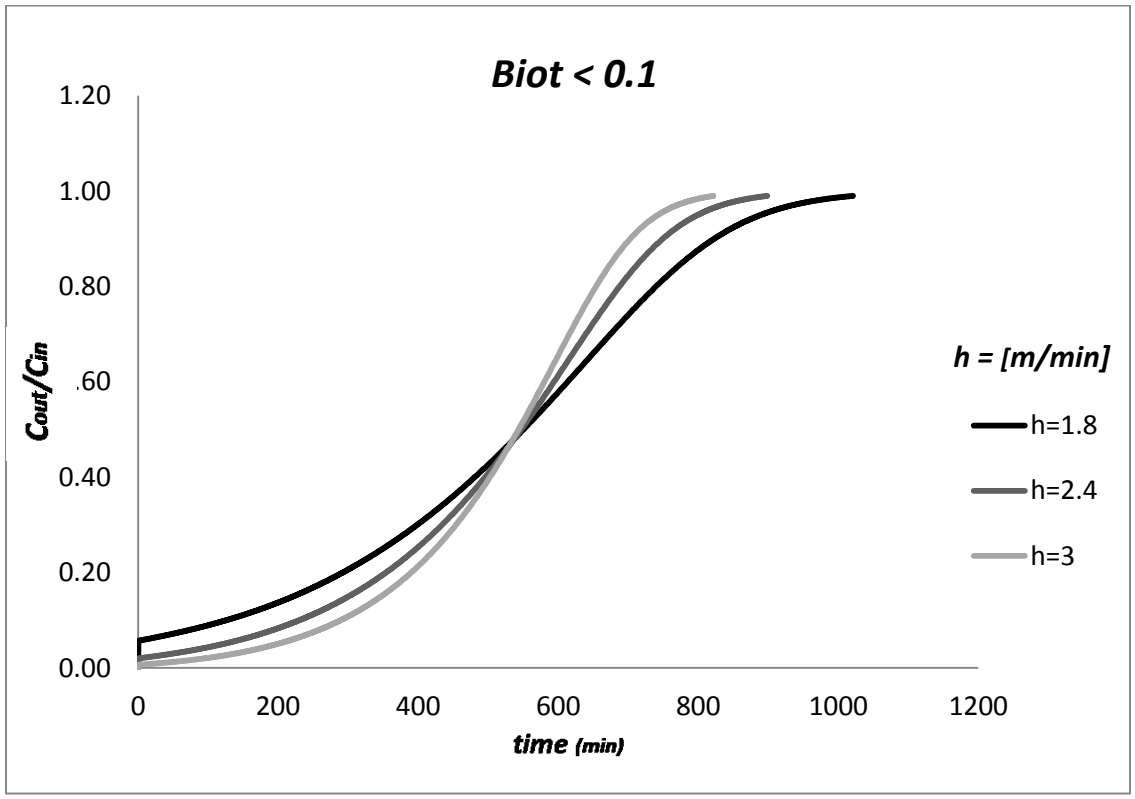

Figure 4-18: Effect of varying the convective mass transfer coefficient for for small Biot number

As anticipated, for small values of Biot number, as the convective mass transfer coefficient increases the initial efficiency increases but the saturation time of the bed decreases.

4.6.2. Diffusivity within the pellets

In this subsection, the diffusion coefficient effect within the pellets is studied. All the input parameters are kept as in Chapter 3 and the diffusivity is taken within two different ranges of order of magnitudes, 10^{-6} and 10^{-8} m^2/s, so as to obtain small and large Biot numbers.

- Large Biot number (Biot >1):

Figure 4-19 shows that, for large Biot number, as the diffusivity within the particles decreases, the initial efficiency decreases and the breakthrough curve starts at a higher value. Besides, as the diffusivity decreases, the breakthrough curve increases slower and the system with lower diffusivity reaches the saturation point slower.

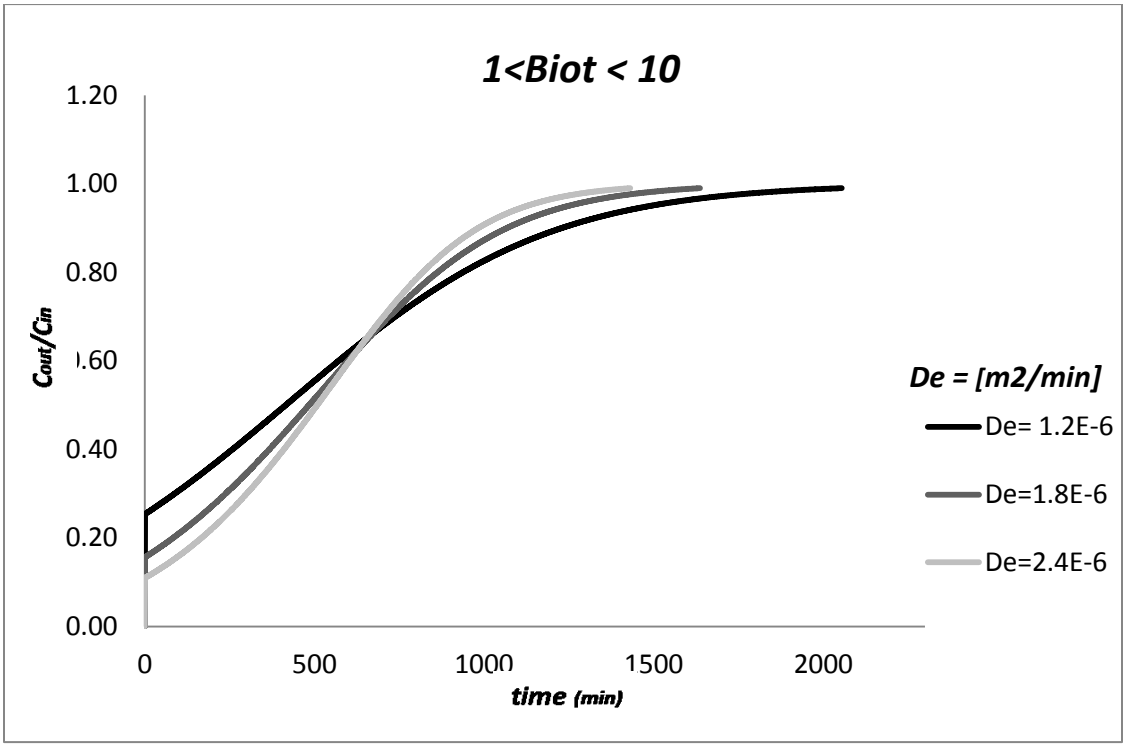

Figure 4-19: Effect of varying the diffusivity within the pellets for large Biot number

- Small Biot number (Biot < 0.1):

  As expected, for small Biot numbers the effect of varying the diffusion coefficient within the particles is negligible. Figure 4-20 shows identical results for different diffusivities in a range of order of magnitude 10^{-6} m^2/s because the controlling resistance for small Biot numbers is the convective mass transfer resistance.

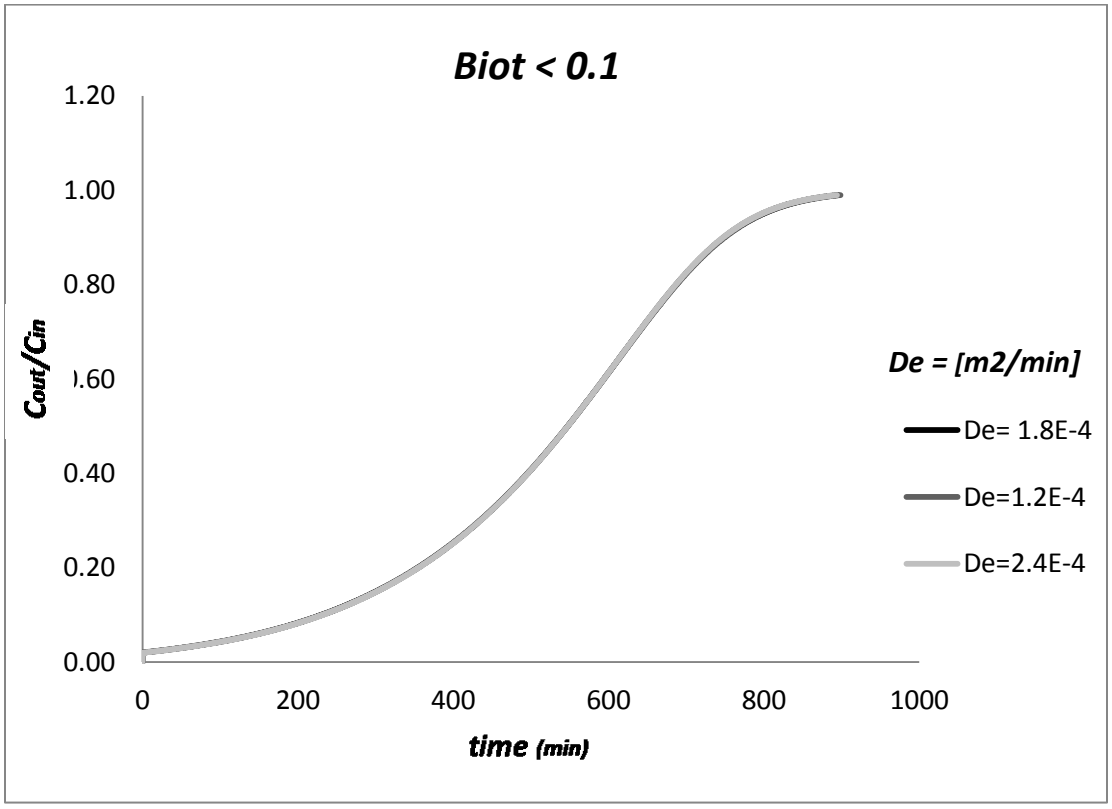

Figure 4-20: Effect of varying the diffusivity within the pellets for small Biot number

4.6.3. Volume flow rate

As mentioned before, to study the effect of different volume flow rates, the effect of changes in the value of convective mass transfer coefficient should be avoided. Therefore the effect of varying the volume flow rate is studied for large Biot number. The input parameters are the same as for small scale tests for MEK, but the volume flow rate (fluid velocity) and

consequently the convective mass transfer coefficient are different for each breakthrough curve.

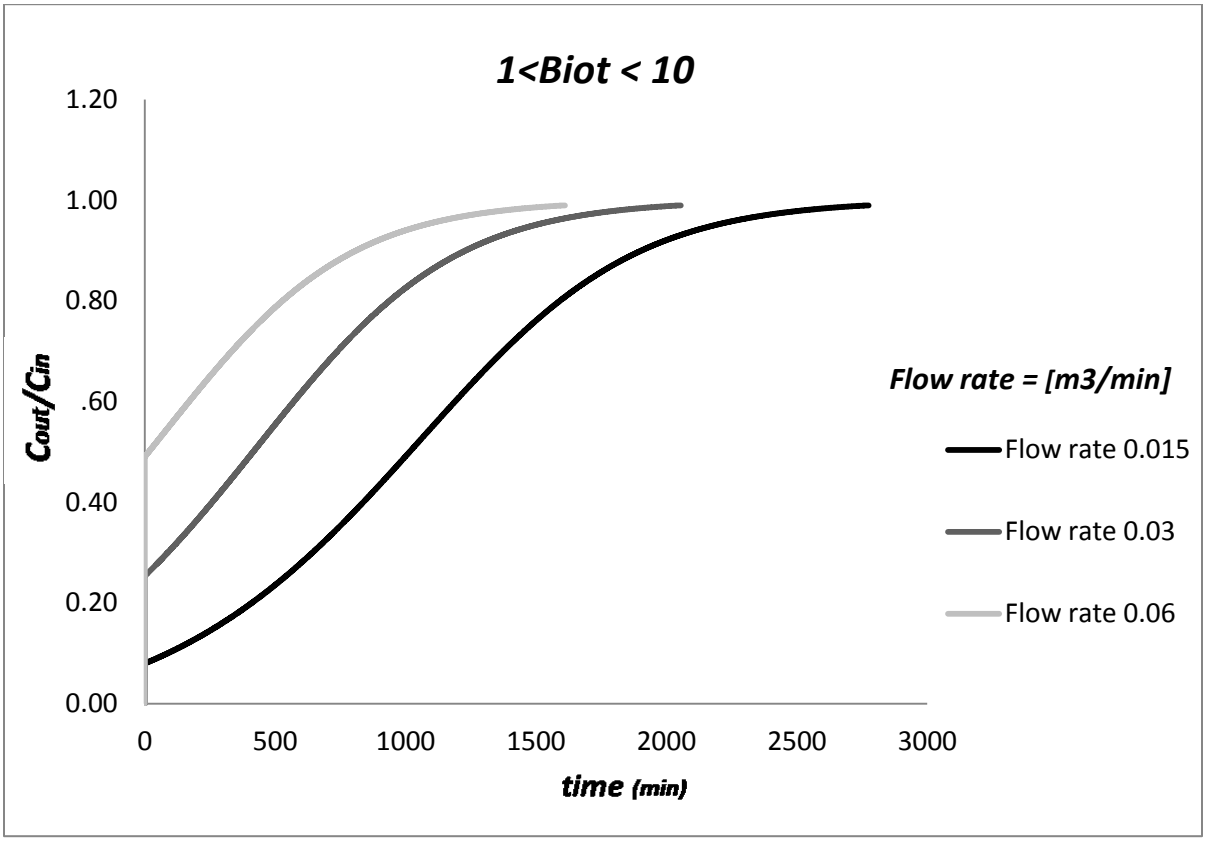

Figure 4-21: Effect of varying the volume flow rate for large Biot number

In Figure 4-21 it is seen that an increase in the volume flow rate results in a decrease in the initial efficiency and a faster saturation because the residence time in the bed decreases as the volume flow rate increases. Although the convective mass transfer coefficient increases with the volume flow rate, as explained before this does not have significant effect on the process for large Biot number and the diagram shows only the effect of the volume flow rate variation.

4.6.4. Size of the pellets

Studying the effect of the pellet size is more complicated than that of previous parameters since it may affect more characteristics. This parameter is also studied for large Biot number

to avoid the effect of variations of the value of the convective mass transfer coefficient. Besides, taking the size of the bed and the mass of the adsorbent to be the same as for small scale tests (Table 3-3), the porosity of the bed is constant and when increasing the pellets diameter the number of particles decreases consequently. Therefore in this section the effect of pellet diameter is studied with fixed bed porosity.

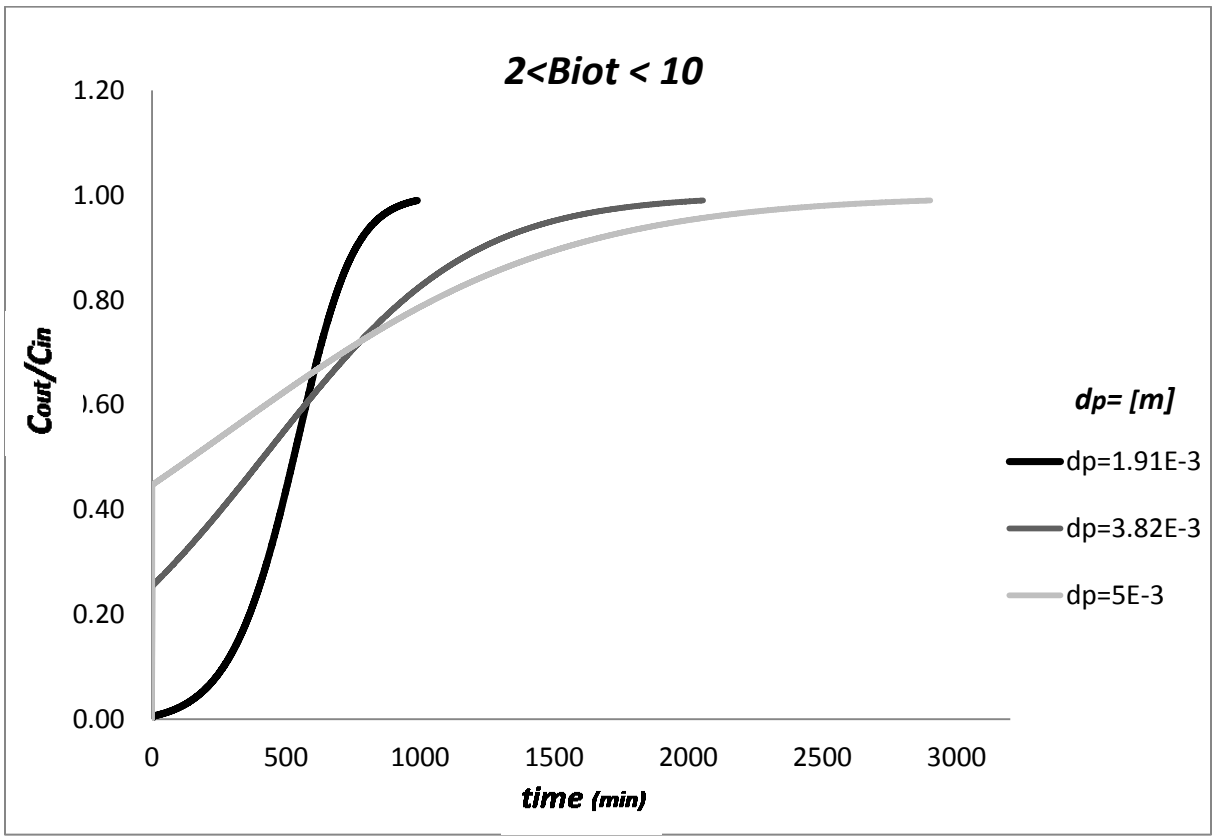

Figure 4-22: Effect of varying the diameter of pellets for large Biot number

Figure 4-22 shows the same effect for an increase in the pellets diameter as for a decrease of the diffusion coefficient within the particle. Indeed increasing the pellet diameter and decreasing the diffusivity within the pellets both have the effect of increasing the diffusion resistance, and therefore result in the same effect on the breakthrough curves. This decreases the initial efficiency at the beginning of the adsorption, however after a certain time the

driving force can overcome the diffusion resistance and mass diffusion starts within the pellets. Thus after a 60% breakthrough it is shown in Figure 4-19 and Figure 4-22 that the particles with higher diffusion resistance (larger diameter or smaller diffusivity) reach the saturation later than the ones with smaller diffusion resistance.

4.7. Sources of error

1. Experimental errors: a complete control of the experimental conditions is not always possible, for example injecting the contaminant so as to keep the inlet concentration constant presents some difficulties in both small and large scale tests.
2. In the model, the particles are assumed spherical, while those used in the experiments are cylindrical (the equivalent spherical diameter is used).
3. Approximation in calculating the diffusivity within the particles where the surface diffusion is neglected.
4. Error in approximating the bed parameters such as the number of particles, porosity and available surface coefficient, etc. using their average value.
5. Round off errors.

Chapter 5: Conclusions

5.1. Summary

A new analytical model is developed to predict the breakthrough curve of the adsorption packed-bed filters. To validate the model, its results are compared with test data obtained from the experimental setup in the Indoor Air Quality Laboratory at Concordia University.

The experiments are categorized as follows:

1. Small scale tests
    - For MEK at l5ppm, 50ppm and 100ppm inlet air concentration
    - For n-hexane at 30ppm, 60ppm and 100ppm inlet air concentration
2. Large scale test for MEK at 18ppm inlet air concentration

For small-scale tests, the model results showed a good agreement in five cases out of six. It predicted rather accurately the performance of the filter for MEK at low and medium levels of inlet air concentration, and for n-hexane at low, middle and high levels of inlet air concentration. Only for high levels of MEK inlet air concentration, namely at 100ppm, discrepancy between the model and the experimental data was found. For a large scale experimental setup the model predicts the breakthrough curve rather well.

In addition, the proposed model is compared with two previously developed models which are representative of the literature on analytical and numerical solutions of the equations governing mass transfer, namely the Rosen model and the Popescu model. The results of these models and the experiments were compared at two levels of inlet concentration for MEK and n-hexane adsorption in a small scale experimental setup as follows:

- For MEK at l5ppm, 50ppm inlet air concentration
- For n-hexane at 60ppm, 100ppm inlet air concentration

The proposed model shows a much better agreement with experiments, which is an appreciable progress with respect to those previous models.

Finally, the effect of some operating parameters is studied, with a specifically-developed method to avoid conflicts between the effects of different parameters. Four parameters were studied as follows:

1. Convective mass transfer coefficient at
    - Large Biot number (Biot > 1)
    - Small Biot number (Biot < 0.1)
2. Diffusivity within the particles at
    - Large Biot number
    - Small Biot number
3. Volume air flow rate at large Biot number
4. Particles diameter at large Biot number

It is shown that, for large Biot number the diffusivity within the particles is the dominant resistance, and that decreasing the diffusion within the pellets decreases the initial efficiency but increases the bed saturation time. For small ranges of Biot number, the convective mass transfer is the limiting process. Thus in small ranges of Biot number, increasing the convective mass transfer coefficient increases the initial efficiency but decreases the bed saturation time.

The effect of varying the volume flow rate and the particle diameter is studied for large Biot number (Biot > 1), in order to prevent perturbations of the results induced by variations of the convective mass transfer coefficient due to changes in Reynolds number. It is concluded that increasing the volume flow rate decreases the bed initial efficiency and also decreases the bed saturation time as it shortens the bed residence time. Increasing the size of the particles has the

same effect as decreasing the diffusion coefficient within the particle since both increase the diffusion resistance.

5.2. Recommendations for future work

1. Adjusting the model for high levels of MEK inlet concentration, tests with non-constant inlet concentration and improving the process time of the code.
2. Validating the model for more experimental conditions such as other types of contaminants or other concentration levels, or even other adsorption systems such as water treatment processes.
3. Studying the effect of varying other operating parameters like the bed porosity, inlet concentration, bed depth, linear adsorption isotherm coefficient, etc.

REFERENCES

ASHRAE . 2004. ANSI/ASHRAE Standard 55-2004: Thermal environmental conditions for human occupancy, American Society of Heating, Refrigerating and Air-Conditioning Engineers, Inc., Atlanta.

ASHRAE Standard 62.1. (2007-b) ventilation for acceptable indoor air quality, American Society of Heating, Refrigerating and Air-Conditioning Engineers, Inc., Atlanta.

Babu, B.V., Gupta S. (2005) Modeling and simulation of fixed-bed adsorption column: effect of velocity variation, J.Eng.Technol, 1: 60-66

Balci, B., Keshinkan, O., Multlu, A. (2011) Ude of BDST and ANN model for prediction of dye adsorption efficiency of Eucalyptus camaldulensis barks in fixed-bed system, Expert Systems with applications, 38: 949-956

Bautista, L.F., Martinez M., Aracil, J. (2003) Adsorption of α-Amylase in a fixed bed: Operating efficiency and kinetic modeling, AIChE Journal, 49 (10): 2631-2641

Bobcock, R.E., Green, D.W., Perry, R.H. (1966). Longitudinal dispersion mechanisms in packed beds, AIChE Journal, 12: 922

Bohart, G.S., Adams, E.Q. (1920). Some aspects of the behavior of charcoal with respect to chlorine, J. Chem. Soc, 42: 523-544

Çengel Y.A., (2007) Heat and Mass Transfer A practice approach, Third edition, McGraw-Hill, New York

Chang, H., Yuan, X., Tian, H., Zeng, Ai-Wu. (2006) Experiment and prediction of breakthrough curves for packed bed adsorption of water vapor on cornmeal, Chemical Engineering and Processing, 45: 747-754

Charles, K., Magee, R.J., Won, D., Lusztyk, E. (2005) Indoor air quality guidelines and standards, Institute for research in construction, National Research Council Canada

Choy, K.K.H., Porter, J.F., McKay, G. (2001). A film-pore-surface diffusion model for the adsorption of acid dyes on activated carbon, Kluwe Academic Publishers, Manufactured in the Netherlands, Adsorption7: 305-317

Do, H.D., Do, D.D., Prasetyo, I. (2001). Surface diffusion and adsorption of hydrocarbons in activated carbon. AIChE Journal, 47(11): 2515-2525

EPA (2000) Energy cost and IAQ performance of ventilation systems and controls, United States Environmental Protection Agency, Indoor Environments Division

Goud, V.V., Mohanty, K., Rao, M.S., Jayakumar N.S. (2005). Prediction of mass transfer coefficients in packed bed using tamarind nut shell activated carbon to remove phenol, Chem. Eng. Technol, 28 (9): 991-997

Hand, D.W., Crittenden, J.C., Hokanson, D.R., Bulloch, J.L. (1997). Predicting the performance of fixed-bed granular activated carbon adsorbers, Water Science and Technology, 35(7): 235-241

Higashi, K., Ito, H., Oishi, J. (1963). Surface diffusion phenomena in gaseous diffusion. I. Surface diffusion of pure gas, J. At. Energy Soc. 5: 846

Inglezakis, V.J., Poulopoulos, S.G. (2006). Adsorption, Ion Exchange and Catalysis Design of Operations and Environmental Applications, Elsevier, Amsterdam, Netherland

Kapoor, A., Yang, R.T. (1991). Contribution of concentration-dependent surface diffusion to rate of adsorption, Chem. Eng. Sci. 46: 1995-2002

Kholafaei, H. (2009). Indoor Air Contaminant Removal: Full-Scale Testing of In-duct Filters, Building, Civil and Environmental Engineering Department, Concordia University, Montreal

Khazraie, A., Kholafaei, H., Haghighat, F., Lee, C. (2011). The effect of relative humidity level, VOC type and multiple VOCs on the performance of full-scale GAC filters, 12th International Conference on Indoor Air Quality and climate, Austin, Texas

Lee, C.S. (2003). A theoretical study on VOC source and sink behavior of porous building material. Ph.D. Thesis, Concordia University, Montreal, Canada.

Miyabe, K., Takeuchi, S. (1997). Model for surface diffusion in liquid-phase adsorption, AIChE Journal, 43: 2997-3006

Masamune, S., Smith, J.M. (1964). Adsorption rate studies significance of pore diffusion, A.I.Ch.E. Journal, 10 (2): 246- 252

Neretniek, I. (1976). Analysis of some adsorption experiments with activated carbon, Chem. Eng.Sci. 31: 1029-1035

Noll, K.E., Gounaris, V., Hou, WS. (1992). Adsorption Technology for Air and Water Pollution Control, Lewis Publishers, Inc., Chelsea, Michigan

Pei, J., Zhang, J. (2010). Modeling of sorbent-based gas filters: Development, verification and experimental validation, Building Simulation, 3(1): 75-86

Petrovic, L.J., Thodos, G. (1968). Mass transfer in the flow of gases through packed bed, I & EC Fundamentals, 7(2): 274-280

Popescu, R.S., Blondeau, P., Jouandon, E., Colda, I. (2007). Breakthrough time of activated-carbon filters used in residential and office buildings- modeling and comparison with experimental data, Proceeding of Clima 2007 Wellbeing Indoors

Pure Water Lab, Mass transfer zone, University of California, San Diego and the University of Arizona, available at: http://purewaterlab.org/pwl_net/labs/D2_Process_Units/D2L4_Activated_Carbon/Mass_Transfer_Zone.html

Ramesh, S.T., Grandhimathi, R., Nidheesh, P.V., Badabhangni, N., Bharathi, K.S. (2011). Breakthrough data analysis of adsorption of Cd (II) on coir pith column, Electronic Journal of Environmental, Agricultural and Food Chemistry, 10(7): 2487-2505

Ranz, W.E., Marshall, W.R., (1952). Evaporation from drops part I, Chemical Engineering Progress, 48(3): 141-146

Ranz, W.E., Marshall, W.R., (1952). Evaporation from drops part II, Chemical Engineering Progress, 48(4): 173-180

Rasmuson, A., Neretnieks, I. (1980). Exact solution of a model for diffusion in particles and longitudinal dispersion in packed beds, AIChE Journal, 26(4): 686-690

Richard, D., Nunez, M.L.D., Schweich, D. (2010). Adsorption of complex phenolic compounds on active charcoal: Breakthrough curves, Chemical Engineering Journal, 158: 213-219

Rosen, J.B. (1952). Kinetics of a fixed bed system for solid diffusion into spherical particles, The Journal of Chemical Physics, 20 (3): 387-394

Ruthven, D M. (1984). Principles of Adsorption and Adsorption Processes, Wiley, New York

Safari, V. (2011). A Systematic Approach to Evaluate Gaseous Filter Models, Building, Civil and Environmental Engineering Department, Concordia University, Montreal

Singh, T.S., Pant, K.K. (2006). Experimental and modeling studies on fixed bed adsorption of As(III) ions from aqueous solution, Separation and Purification Technology, 48: 288-296

Sze, M.F.F., Lee, V.K.C, McKay, G. (2008). Simplified fixed bed column model for adsorption of organic pollutants using tapered activated carbon columns, Desalination, 218: 323-333

Thoenes, D., Kramers, H. (1958). Mass transfer from spheres in various regular packing to a flowing fluid, Chemical Enginnering Science, 8: 271-283

Wakao, N., Funazkri, T. (1978). Effect of fluid dispersion coefficients on particle to fluid mass transfer coefficient in packed beds, Chemical Engineering Science, 33: 1375-1384

Walker, G.M., Weatherley, L.R. (1997) Adsorption of acid dyes on to granular activated carbon in fixed beds, Wat. Res, 31(8):2093-2101

Whitaker, S. (1972). Forced convection heat transfer correlations for flow in pipes, past plates, single cylinders, single spheres, and for flow in packed beds and tube bundles, AIChE Journal, 18 (2): 361-371

Xu, Q., Zhang, Y., Mo, J., Li, X. (2011) A new method to evaluate the performance of adsorbents for indoor VOCs purification, 12th International Conference on Indoor Air Quality, Austin, Texas

Yang, Ralph T., Ed. (1997). Gas Separation By Adsorption Processes, Imperial college Press, London

Yang, X., Otto, S.R., Al-Duri, B. (2003). Concentration-dependent surface diffusivity model (CDSDM) numerical development and application, Chemical Engineering Journal, 94: 199-209

Yin, C.Y., Aroua, K., Duad, W.M.A.W. (2009) Fixed-bed adsorption of metal ions from aqueous solution on polyethyleneimine-impregnated palm shell activated carbon, chemical Engineering Journal, 148: 8-14

Young D.M., Crowell A.D. (1962) Physical Adsorption of Gases, Butterworth, London

Zhao, M., Duncan, J.R. (1998). Bed-depth-service-time analysis on column removal of Zn^{2+} using Azolla filiculoides, Biotechnology Letters, 20(1): 37-39